Energy evaluation of R152a as drop in replacement for R134a in cascade refrigeration plants.

R. Cabello [a*], D. Sánchez [a], R. Llopis [a], J. Catalán[a], L. Nebot-Andrés[a], E. Torrella [b]

[a]*Universitat Jaume I, Dep. of Mechanical Engineering and Construction, Campus de Riu Sec s/n E-12071, Castellón, Spain*

[b]*Universitat Politècnica de València, Department of Applied Thermodynamics, Camino de Vera, 14, E-46022, Valencia, Spain*

*Corresponding author: R. Cabello (cabello@uji.es), Phone: +34 964 72 8135; Fax: +34 964 728106.

ABSTRACT

An experimental comparison has been performed of a cascade refrigeration facility working with therefrigerant pairs R134a/R744 and R152a/R744. This kind of facility is suitable for industrial and commercial refrigeration applications. The high GWP refrigerant R134a has been substituted with the low GWP refrigerant R152a, in accordance with the new environmental regulations aimed at mitigating the Greenhouse effect. As both refrigerants belong to the family of HFC fluids, the replacement has been carried out as a drop-in. Apart from safety considerations, as R152a is included in the A2 group, the results of the wide range of tests conducted show that no special energy improvement or worsening is achieved, and that the replacement of R134a with R152a is technically and energetically feasible.

KEYWORDS

R152a, R134a, CO_2, Low GWP refrigerants, Cascade refrigeration system.

NOMENCLATURE

COP	coefficient of performance
c_p	specific isobaric heat, kJ·kg^{-1}·K^{-1}
GWP	global warming potential (100 years integration)
h	specific enthalpy, kJ·kg^{-1}
HOC	Heat of combustion
HTC	high temperature cycle
LTC	low temperature cycle
MW	Molecular weight kg·kmol^{-1}
$\dot{m}$	mass flow rate, kg·s^{-1}
N	Compressor speed (r.p.m.)
NBP	Normal boiling point
p	pressure, bar
P_C	compressor power consumption, kW
$\dot{Q}$	heat transfer rate, kW
q_o	Specific cooling capacity (kJ/kg)
q_v	Volumetric refrigerating effect (kJ/m^3)
SF	secondary fluid
t	pressure ratio
T	temperature, ºC
v	specific volume, m^3·kg^{-1}
$\dot{V}$	Volumetric flow rate, m^3·h^{-1}
$\dot{V}_G$	Compressor displacement, m^3·s^{-1}
w_c	specific compression work, kJ·kg^{-1}
w_{cs}	isentropic specific compression work, kJ·kg^{-1}
x_v	vapor quality

GREEK SYMBOLS

Δ	Increment
λ	latent heat (kJ/kg)
η_G	compressor global efficiency
η_s	compressor isentropic efficiency
η_v	compressor volumetric efficiency

ρ	density, $kg \cdot m^{-3}$

SUBSCRIPTS

casc	Cascade
crit	critical
dis	Discharge
env	environment
H	high-temperature cycle
k	condensing level
L	low-temperature cycle
o	evaporating level
ref	Refrigerant
s	Isentropic
sf	Secondary fluid
suc	Suction

1. Introduction

Guided by UNEP and IPCC reports, a global warming limit of 2 ºC or below (relative to pre-industrial levels) has been adopted as a threshold for mitigation efforts targeted toward reducing climate change risks, impacts and damage [IPCC (2014); European Commission (2005); M. Meinshausen et al. (2009)].

Accordingly, new regulations regarding fluorinated gases (F-Gases) are being approved, with the aim of achieving a reduction in the use and commercial availability of this kind of gases when their GWP present a high value. A clear example is Regulation EU nº 517/2014 [European Commission (2014)] passed in the European Union. This Regulation establishes, among other restrictions, a 79% reduction in the amount of hydrofluorocarbons to be placed on the market by the year 2030 with respect to the annual average of the total amount placed on the market in the Union during the period from 2009 to 2012. Moreover, in European countries like Spain, new laws have come into force that impose taxes on the F-Gases with GWP values higher than 150 [Law (2013); RD (2013)].

Section 13 of *Annex II* of Regulation EU no 517/2014 imposes a ban on placing multipack centralized refrigeration systems on the market for commercial use if they have a rated capacity of 40 kW or more and contain, or whose functioning relies upon, fluorinated greenhouse gases with a GWP of 150 or more. An exception to this ruling is in the primary refrigerant circuit of cascade systems, where fluorinated greenhouse gases with a GWP below 1500 may be used.

Nowadays, the refrigeration systems mounted for commercial applications normally use the working fluids R134a, R404A and R507A in direct expansion systems [Kauffeld (2008), Arora and Kaushik (2008)]. Their GWP values are 1300, 3943 and 3985 respectively, as published in the Assessment Report 5 of the Working Group I [IPCC (2013)], which means that those refrigeration systems must be either retrofitted or replaced with new ones adapted to the refrigerants allowed by Regulation EU no 517/2014 (HFC with low GWP, HFOs, Hydrocarbons, CO_2 and ammonia) [M. Mohanraj et al. (2009); AREA (2011); W. Goetzler et. Al. (2014); JM. Calm (2008)].

The refrigeration technologies for commercial applications, with medium and high cooling capacity demands, that best suit the refrigerants allowed by the Regulation mentioned above are the following multi-stage vapor compression ones: Transcritical CO_2 booster system with direct expansion, direct cascade and indirect cascade. Both cascade types uses subcritical CO_2 in direct expansion for low temperature, but the direct one works in direct expansion for medium temperature and the indirect one works with a secondary fluid for medium temperature [O. Abdelaziz (2012); Vishaldeep et al. (2014); M. Beshr et al. (2015), R. Llopis et al. (2015,a)].

The present paper is focused on the experimental comparison of a direct cascade refrigeration plant working with the refrigerant pairs R134a/R744 and R152a/R744 under a wide range of operating conditions. The results are a valuable contribution to the experimental knowledge on this kind of refrigeration plants, especially because no data with R152a can be found in the literature. R152a is a low GWP refrigerant, with a reduced price compared to other HFC and HFO refrigerants, and is included in the A2 safety group following the ASHRAE Std32 [ASHRAE (2013)] designation. The results revealed the technological feasibility of using R152a as a replacement fluid for R134a, without any detrimental effect on the energy performance of the plant. Safety considerations are not within the scope of this work.

2. Refrigerant Comparison

The basic properties of R152a and R134a are shown in Table 1. The data shown in this table are taken from a paper published by R. Cabello et al. (2015), where different aspects of these two refrigerants are discussed. Thermodynamic properties are calculated using the software application REFPROP v9.1 [Lemmon et al. (2013)], the Safety Group is in accordance with ASHRAE Std-34 [ASHRAE (2013)], HOC and RCL values are extracted from [Calm (2012)], and GWP values are taken from [IPCC (2013)].

Fluid	Chemical formula	P_{crit} (MPa)	T_{crit} (ºC)	MW (kg·kmol^{-1})	NBP (ºC)	$v_{sat,v}$* (m^3·kg^{-1})	λ* (kJ·kg^{-1})	qv* (kJ·m^{-3})	Safety Group	RCL (gr·m^{-3})	HOC (MJ·kg^{-1})	GWP[1] WGI-AR5[1]
R152a	CH_3CHF_2	4.52	113.26	66.051	-24.02	0.296	329.91	1113.66	A2	32	17,4	138
R134a	CH_2FCF_3	4.06	101.06	102.032	-26.07	0.190	216.97	1140.81	A1	210	4.2	1300

[1]Working Group I contribution to the IPCC Fifth Assessment Report

*property calculated at NBP

Table 1 – Main thermodynamic, safety and environmental properties of R134a and R152a

Both refrigerants are HFC, but the first issue to comment on is the GWP value of R152a, which is below 150. This means that R152a is beyond the scope of the new regulations related to F-Gases, so no reductions, replacements, prohibitions or taxes should be applied to this fluid. This is not the case of R134a, which has a higher GWP (1300) and the new F-Gas regulations apply.

The molecules of R134a and R152a are derived from the ethane molecule, and consist of the same type of atoms (hydrogen, carbon and fluorine) and the same kind of bonds between them, so the material and lubricant compatibility is the same for both refrigerants. Therefore, R152a could be a drop-in replacement for R134a. However, the increased presence of hydrogen atoms at the expense of fluorine atoms in the R152a molecule with respect to that of R134a is the main drawback of R152a compared with R134a, because it generates a higher flammability, to the extent that R152a meets ASHRAE Std 34 criteria for A2 status.

Both refrigerants present a similar NBP and critical point and therefore both can be used in the same temperature range. Notwithstanding, the latent heat and specific volume of R152a are much greater than R134a.

On the one hand, the higher latent heat of R152a than that of R134a will imply that its mass flow rate will be smaller to obtain the same cooling duty, which will have a bearing on lesser compressor power consumption. On the other hand, the higher specific volume of R152a with respect to R134a will mean that less refrigerant mass will need to be charged in the facility in order to reach the same saturation temperatures. The result of dividing the latent heat between the specific volume, named volumetric refrigerating effect (q_v), yields values that are 10%y greater for R134a than for R152a, which means that the compressor dimensioned for R134a will be slightly smaller for R152a if the same cooling duty is to be obtained.

3. Cascade Theoretical study

First we present an approximate theoretical study of a cascade cycle working with the refrigerant pairs R134a/R744 and R152a/R744, in order to check the discrepancies, if any, between the theoretical and the actual behavior of a cascade refrigeration cycle. The starting data to calculate the cycle are given in Table 2.

	High Temperature Cycle (HTC)	Low Temperature Cycle (LTC)
Working Fluid	HFC134a	R744 (CO_2)
	HFC152a	
Evaporating Temperature (ºC)	-	T_{oL}= -30
Condensing temperature (ºC)	T_{kH} =30	T_{kL} =-7
Superheat at evaporator outlet (K)	5	5
Subcooling at expansion valve inlet (K)	2	2
Superheat at compressor suction (K)	15	15
Isentropic efficiency*	$\eta_s = 1 - 0{,}02 \cdot \frac{p_k, H}{p_{O,H}}$	$\eta_s = 1 - 0{,}04 \cdot \frac{p_k, L}{p_{O,L}}$
Volumetric efficiency*	$\eta_v = 1 - 0{,}02 \cdot \frac{p_k, H}{p_{O,H}}$	$\eta_v = 1 - 0{,}04 \cdot \frac{p_k, L}{p_{O,L}}$
Refrigeration load $(\dot{Q}_{O,L}, kW)$	1	
$\Delta T_{casc.}$ (K)	5	

Table 2. Input data for theoretical simulation.

**These linear correlations of the compressor efficiencies with the pressure ratio are taken from the literature, for instance W.B.Gosney 1982 and E. Granryd 2009. Meanwhile, the particular coefficients and constants used in the correlations are taken from author's experience.*

The value of the LTC parameters are equal regardless of the refrigerant considered in HTC, which means there will be the same evaporation temperature at the HT and the same ΔT_{casc}. for both refrigerants. Thermodynamic properties have been calculated by means of the software application REFPROPv9.1 [Lemmon et al. (2013)]. The corresponding R134a/R744 and R152a/R744 cycles are shown in Figure 1, where LTC is depicted in a vanished gray color, and HTC for R134a and R152a are depicted in red and green respectively.

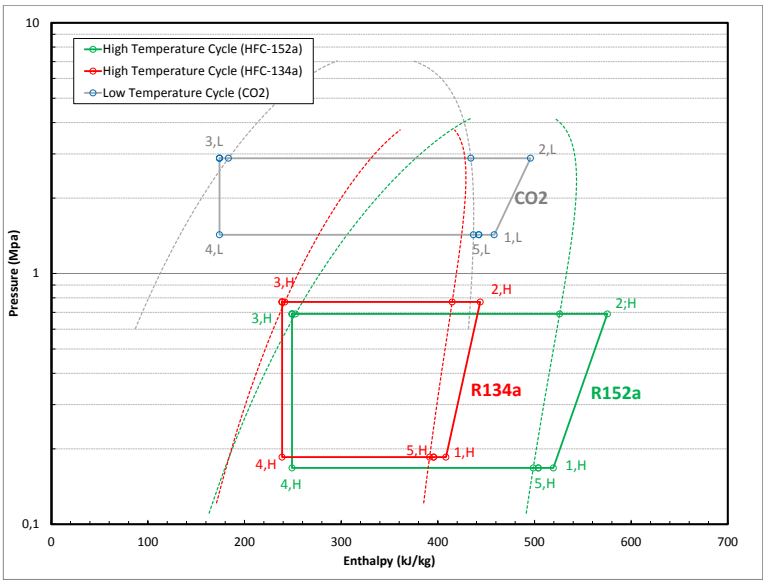

Figure 1. Comparison of the theoretical cascade cycles for R134a/R744 and R152a/R744.

Once the thermodynamic properties have been calculated, the main energy parameters are obtained using the set of equations shown in Table 3. There is a correspondence between subscripts in the equations and those in the cycles depicted in Figure 1. The results of the energy parameters calculated are shown in Table 4.

$q_o = h_5 - h_4$	Eq (1)	$q_v = \frac{q_o}{v_1}$	Eq (2)
$\dot{m}_{ref,L} = \frac{\dot{Q}_{o,L}}{q_{o,L}}$	Eq (3)	$\dot{m}_{ref,H} = \frac{\dot{m}_{ref,L} \cdot (h_{2L} - h_{3L})}{q_{o,H}}$	Eq (4)
$\dot{V}_G = \frac{\dot{m}_{ref} \cdot v_1}{\eta_v}$	Eq (5)	$w_{c,s} = h_{2s} - h_1$	Eq (6)
$w_c = \frac{h_{2s} - h_1}{\eta_i}$	Eq (7)	$P_C = \dot{m}_{ref} \cdot w_c$	Eq (8)
$t = \frac{p_k}{p_o}$	Eq (9)	$COP_L = \frac{h_{5L} - h_{4L}}{h_{2L} - h_{1L}}$	Eq (10)
$COP_H = \frac{h_{5H} - h_{4H}}{h_{2H} - h_{1H}}$	Eq (11)	$COP_{casc.} = \frac{\dot{m}_{ref,L} \cdot (h_{5L} - h_{4L})}{\dot{m}_{ref,L} \cdot (h_{2L} - h_{1L}) + \dot{m}_{ref,H} \cdot (h_{2H} - h_{1H})}$	Eq (12)

Table 3. Equations used in the theoretical simulation.

HTC results with R152a			HTC results with R134a		
$\dot{m}_{ref,H}$	(kg/s)	0.0047	$\dot{m}_{ref,H}$	(kg/s)	0.0076
$q_{o,H}$	(kJ/kg)	254.7	$q_{o,H}$	(kJ/kg)	156.8
$q_{v,H}$	(kJ/m^3)	1264.4	$q_{v,H}$	(kJ/m^3)	1331,8
$\dot{V}_{G,H}$	(m^3/s)	0.00103	$\dot{V}_{G,H}$	(m^3/s)	0.00098
$w_{c,s,H}$	(kJ/kg)	51.3	$w_{c,s,H}$	(kJ/kg)	32.6
$w_{c,H}$	(kJ/kg)	55.9	$w_{c,H}$	(kJ/kg)	35.5
$Pc,_H$	(W)	263	$Pc,_H$	(W)	271
$T_{dis,H}$	(K/ºC)	342.3 / 69.2	$T_{dis,H}$	(K/ºC)	316.0 / 42.9
t_H	-	4.11	t_H	-	4.15
COP_H	-	3.6	COP_H	-	3.3
LTC results with R744					
$\dot{m}_{ref,L}$	(kg/s)	0.0037			
$q_{o,L}$	(kJ/kg)	268.3			
$q_{v,L}$	(kJ/m^3)	8738.9			
$\dot{V}_{G,L}$	(m^3/s)	0.00012			
$w_{c,s,L}$	(kJ/kg)	33.3			
$w_{c,L}$	(kJ/kg)	37.6			
$Pc,_L$	(W)	140			
$T_{dis,L}$	(K/ºC)	316.6 / 42.9			
t_L	-	2.40			
COP_L	-	5.0			
COP_{casc}	(R152a/CO_2)	2.480	COP_{casc}	(R134a/CO_2)	2.430

Table 4. Energy parameters calculated.

Focusing on the HTC results shown in Table 4, the specific cooling capacity (q_o) is much greater for R152a than for R134a, which results in a substantial reduction in the mass flow rate for the same cooling duty. Notwithstanding, this reduction in mass flow rate does not lead to a reduction in the compressor power consumption, because it is offset by a higher isentropic specific work (w_c), and both refrigerants generate a very similar P_{cH} value.

The pressure ratio in HTC is practically equal for both refrigerants, so assuming the volumetric efficiency to be a function mainly of this parameter, R134a and R152a present the same value of η_v. In accordance with Equation 5, the compressor displacement should be higher (5% under the conditions simulated) if the plant works with R152a than if it works with R134a, since the reduction in mass flow rate is offset by the higher value in suction specific volume.

Finally, the slightly higher compressor power consumption for R134a than for R152a, and the equal $\acute{Q}_{OL}$ value considered for both refrigerants results in a slightly higher COP value for R152a.

4. Experimental facility

The experimental plant, which can be seen in Figure 2, corresponds to an R134a/R744 cascade refrigeration system designed to operate at the low evaporating temperature level of commercial refrigeration (-40 to -30 ºC). The plant is driven by two single-stage reciprocating compressors: a CO_2 variable speed semi-hermetic compressor for subcritical applications, with a displacement of 3.48 m^3/h at 1450 rpm and a nominal power of 1.5 kW, which drives the LT cycle, and a variable speed semi-hermetic compressor, with a displacement of 32.66 m^3/h at 1450 rpm and nominal power of 3.7 kW, dimensioned for R134a, which drives the single-stage HT cycle. The heat exchangers are of the brazed plate type with heat transfer surface areas of 2.39m^2 for the HT condenser, 2x1.76m^2 for cascade condensers and 2.39m^2 for the LT evaporator. The facility incorporates electronic expansion valves. Figure 3 shows the schematic diagram of the plant, the position of the measurement devices and the designation. Next, we present the details of the plant, of the thermal support system and of the measurement instrumentation.

Figure 2. View of the cascade refrigeration plant.

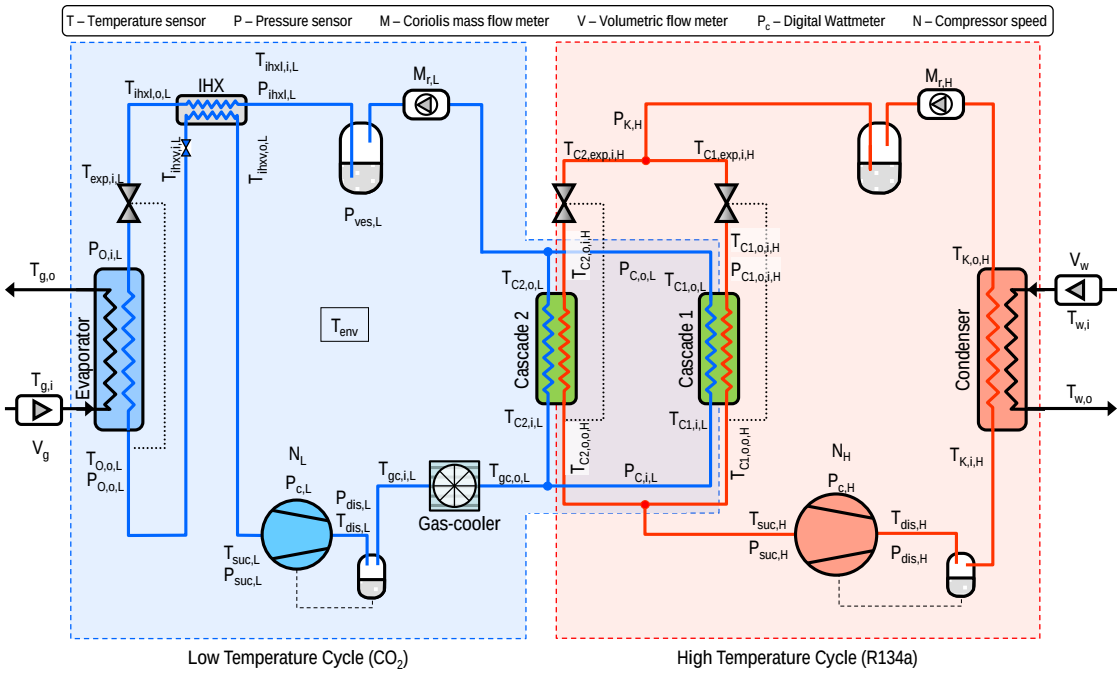

Figure 3. Schematic diagram of the experimental plant.

A more detailed description of the refrigeration facility, including the main characteristics of all the measurement instruments and their accuracies, can be obtained in C. Sanz-Kock et al. (2014), R. Llopis et al. (2015,b), and R. Llopis et al. (2016).

5. Test campaign

The R134a experimental results were extracted from the work published by Sanz-Kock et al. (2014). For comparison purposes, new tests were conducted with R152a in the same refrigeration facility, maintaining the same operating conditions.

The replacement of R134a with R152a was performed as a drop-in, and no changes were made in the facility or the lubricant. For a proper regulation of the electronic expansion valves, the R152a saturation curve was programmed in the expansion valve controller.

5.1 Experimental procedure

In order to conduct the tests, cascade refrigeration cycles present three degrees of freedom: HT condensing temperature ($T_{k,H}$), LT evaporating temperature ($T_{o,L}$), and temperature difference in the cascade condenser (ΔT_{casc}).

For both refrigerants, the test campaign carried out to evaluate the performance of the cascade refrigeration system covered LT evaporating temperatures from -40 to -30 ºC and HT condensing temperatures from 30 to 50 ºC, these values being regulated and maintained by the secondary fluid loop

systems. To perform ΔT_{casc} variations, for each combination of T_{kH} and T_{oL} temperatures (9 tests), the operation of the cascade was registered regulating the HT compressor speed (five values). The LT compressor speed was maintained at its nominal value, because of its poor global efficiency, as explained in Sanz-Kock et al. (2014). Tests were carried out fixing 10 ºC of superheat in the expansion valves that feed the cascade condensers and the LT evaporator. Furthermore, the fan of the gas-cooler was always kept on, with a a constant consumption value of 75 W.

Altogether, 45 steady-states of the plant were measured for each refrigerant, each lasting at least 20 minutes, with a sampling rate of 5 seconds and a maximum oscillation of the phase-change temperatures of 2%, as detailed in Tables 5a and 5b.

$T_{o,L}$	$T_{k,L}$	$\Delta T_{SH,L}$	N_L	$T_{o,H}$	$T_{k,H}$	$\Delta T_{SH,H}$	T_{env}	N_H	Steady-states
(ºC)	(ºC)	(ºC)	(rpm)	(ºC)	(ºC)	(ºC)	(ºC)	(rpm)	
-30 ± 0,1	-6.6 to -0.6	9.3 ± 0.2	1450	-10.9 to -4.4	30 ± 0.1	7.4 ± 0.2	27.5 ± 1	705 to 1108	5
-35 ± 0,1	-10.7 to -5.3	9.3 ± 0.1	1450	-15.7 to -9.9	30 ± 0.1	7.7 ± 0.3	26.2 ± 1.8	806 to 1209	5
-40 ± 0,1	-13.2 to -7.9	9.3 ± 0.1	1450	-19.3 to -13.6	30 ± 0.1	8.4 ± 0.3	27.1 ± 1.5	806 to 1209	5
-30 ± 0,1	-6.1 to -1.6	9.2 ± 0.2	1450	-9.6 to -4.2	40 ± 0.1	7.4 ± 0.5	29.9 ± 2	806 to 1209	5
-35 ± 0,1	-9.2 to -3.8	9.2 ± 0.1	1450	-13.4 to -7.7	40 ± 0.1	7.6 ± 0.3	30.0 ± 1.3	806 to 1209	5
-40 ± 0,1	-12.1 to -7.0	9.2 ± 0.1	1450	-17.6 to -11.7	40 ± 0.1	7.8 ± 0.3	29.1 ± 1.6	806 to 1209	5
-30 ± 0,1	-4.6 to 0.9	9.1 ± 0.1	1450	-7.8 to -2.0	50 ± 0.1	7.4 ± 0.2	28.0 ± 1.2	806 to 1209	5
-35 ± 0,1	-7.6 to -2.2	9.1 ± 0.1	1450	-11.6 to -5.7	50 ± 0.1	7.6 ± 0.2	26.7 ± 1.0	806 to 1209	5
-40 ± 0,1	-11.4 to -7.6	9.1 ± 0.1	1450	16.8 to -12.4	50 ± 0.1	7.9 ± 0.2	27.9 ± 1.2	1007 to 1409	5

Table 5a. Summary of the operating conditions maintained during tests performed with the cascade refrigeration plant using R152a/CO_2.

$T_{o,L}$	$T_{k,L}$	$\Delta T_{SH,L}$	N_L	$T_{o,H}$	$T_{k,H}$	$\Delta T_{SH,H}$	T_{env}	N_H	Steady-states
(ºC)	(ºC)	(ºC)	(rpm)	(ºC)	(ºC)	(ºC)	(ºC)	(rpm)	
-30 ± 0,1	--4.9 to 0.2	9.0 ± 0.2	1450	-9.17 to -3.43	30 ± 0.1	8.7 ± 0.8	27.5 ± 1.6	907 to 1310	5
-35 ± 0,1	-6.7 to -0.3	9.0 ± 0.2	1450	-11.29 to -3.50	30 ± 0.1	10.0 ± 0.5	26.6 ± 0.9	705 to 1209	5
-40 ± 0,1	-11.5 to -4.8	9.0 ± 0.2	1450	-17.10 to -9.52	30 ± 0.1	9.5 ± 1.8	24.3 ± 1.3	806 to 1409	5
-30 ± 0,1	-6.9 to -1.6	9.4 ± 0.4	1450	-10.68 to -5.00	40 ± 0.1	9.5 ± 0.6	21.8 ± 1.3	806 to 1209	5
-35 ± 0,1	-11.0 to -6.3	9.3 ± 0.3	1450	-15.29 to -10.28	40 ± 0.1	9.4 ± 0.5	21.4 ± 1.4	907 to 1310	5
-40 ± 0,1	-12.8 to -8.0	9.3 ± 0.1	1450	-17.96 to -12.49	40 ± 0.1	9.6 ± 0.4	20.7 ± 0.7	806 to 1209	5
-30 ± 0,1	-9.2 to -3.8	9.3 ± 1.1	1450	-12.71 to -7.25	50 ± 0.1	10.5 ± 1.2	22.7 ± 0.7	806 to 1209	5
-35 ± 0,1	-12.2 to -7.2	9.5 ± 0.4	1450	-16.03 to -10.57	50 ± 0.1	9.7 ± 1.1	20.9 ± 1.4	806 to 1209	5
-40 ± 0,1	-15.4 to -10.3	9.4 ± 0.1	1450	-20.15 to -14.43	50 ± 0.1	9.4 ± 0.9	20.0 ± 1.1	806 to 12097	5

Table 5b. Summary of the operating conditions maintained during tests performed with the cascade refrigeration plant using R134a/CO_2.

Because a compressor dimensioned for R134a was mounted in the HT cycle and due to the greater specific volume of R152a with respect to R134a, the tests using R152a do not cover exactly the same compressor speed range, but there is sufficient overlap in both ranges to carry out the comparison.

5.2 Data validation

Data validation was carried out by comparing the heat transfer rates for the two fluid sides, in the main heat exchangers of the plant. The Equation 13 calculates the heat transfer rate dissipated from the refrigerant to the water at the HTC condenser, while the Equation 14 calculates the heat transfer rate absorbed by the water at the same heat exchanger.

$$\acute{Q}_{K,H} = \acute{m}_{ref,H} \cdot \left(h_{k,i,H} - h_{k,o,H}\right) \qquad \text{Eq. 13}$$

$$\acute{Q}_{w} = \acute{V}_{w} \cdot \rho_{w} \cdot c_{p,w} \cdot \left(T_{w,o} - T_{w,i}\right) \qquad \text{Eq. 14}$$

Equations 15 and 16 are used to calculate the heat transfer rate of rejection and absorption in the cascade heat exchanger, respectively. Due to the presence of two cascade condensers at the facility working in parallel (see figure 3), we have averaged the enthalpy difference of both cascade condensers.

$$\acute{Q}_{K,L} = \acute{m}_{ref,L} \cdot 0{,}5 \cdot \left[\left(h_{C1,k,i,L} - h_{C1,k,o,L}\right) + \left(h_{C2,k,i,L} - h_{C2,k,o,L}\right)\right] \qquad \text{Eq. 15}$$

$$\acute{Q}_{O,H} = \acute{m}_{ref,H} \cdot 0{,}5 \cdot \left[\left(h_{C1,O,o,H} - h_{C1,O,i,H}\right) + \left(h_{C2,O,o,H} - h_{C2,O,i,H}\right)\right] \qquad \text{Eq. 16}$$

With equations 17 and 18 is determined the cooling load provided by the secondary fluid and the heat transfer rate absorbed by the refrigerant at the evaporator

$$\acute{Q}_{sf} = \acute{V}_{sf} \cdot \rho_{sf} \cdot c_{p,sf} \cdot \left(T_{sf,i} - T_{sf,o}\right) \qquad \text{Eq. 17}$$

$$\acute{Q}_{O,L} = \acute{m}_{ref,L} \cdot \left(h_{O,o,L} - h_{O,i,L}\right) \qquad \text{Eq. 18}$$

In Figures 6a and 6b red dots are used to represent the heat transfer rate balance at the HT condenser using Equations 13 and 14, green diamonds represent the heat transfer rate balance at the cascade condenser using Equations 15 and 16, and blue squares represent the heat transfer rate balance at the LT evaporator using Equations 17 and 18.

Regarding the heat balance at the HT condenser, 99.6% of the values present a deviation below ±10%, at the cascade heat exchanger 97.0% of data are within ±10%, and 92.4% of the data in the LT evaporator deviate less than ±10%.

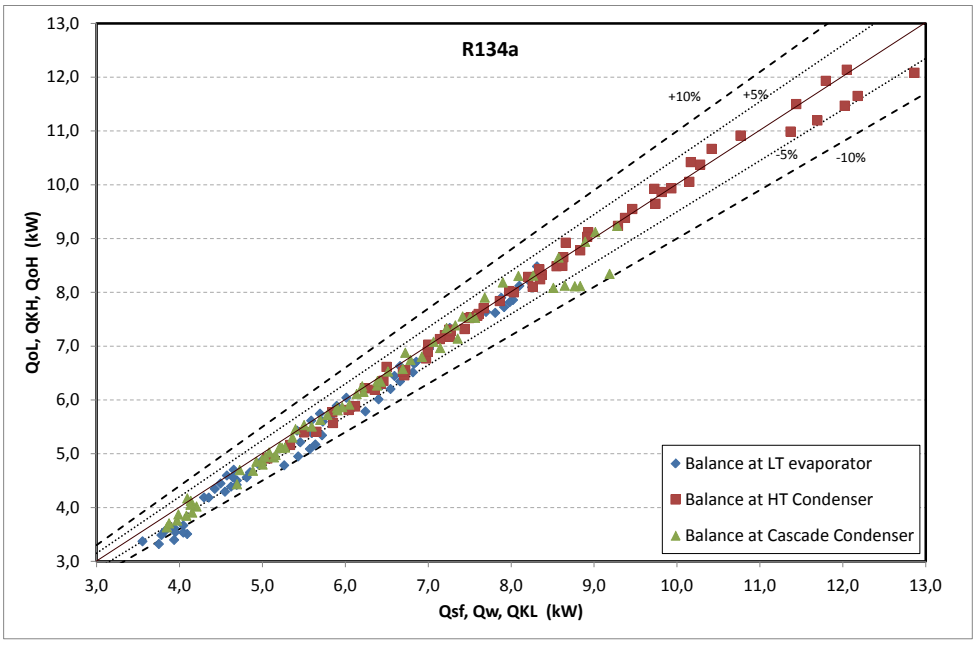

Figure 4a. Validation of heat transfer rates in the cascade plant using R134a/R744.

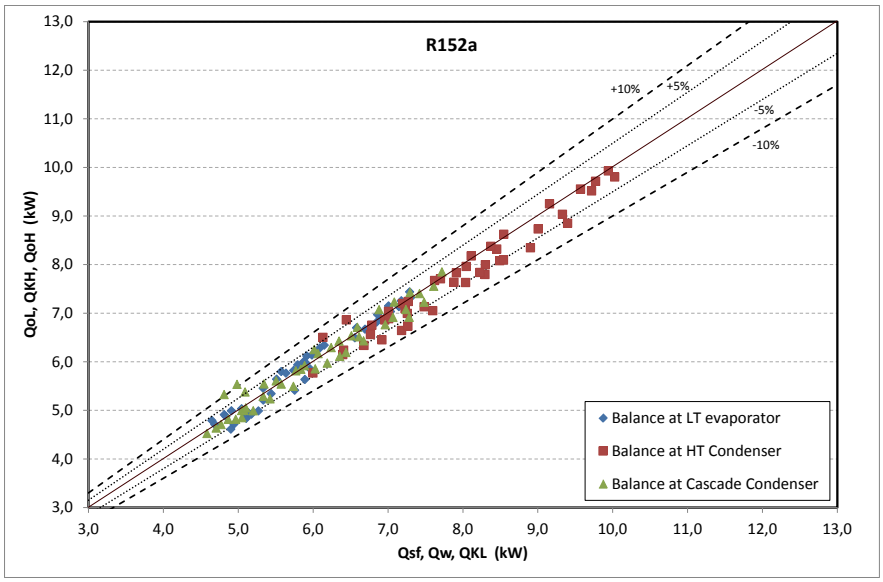

Figure 4b. Validation of heat transfer rates in the cascade plant using R152a/R744.

The heat transfer rate balances show good concordance in both fluids for each heat exchanger, which confirms the accuracy of the measurements.

6. Results and discussion

In order to obtain greater clarity, the analysis is performed showing the results for the two extreme operating conditions, which are when the temperature difference between the heat sink and the cold source are maximum (T_{kH}=50ºC and T_{oL}=-40ºC) and minimum (T_{kH}=30ºC and T_{oL}=-30ºC).

When the operating conditions are the same, we have measured that the CO_2 mass flow rate is practically the same, regardless of the refrigerant charged in the HT cycle. Nevertheless, due to the difference in specific volume, for the same compressor displacement and the same operating conditions, the R134a mass flow rate is nearly twice that of R152a. This difference is practically constant for all the operating conditions tested.

Regarding the $\Delta T_{casc.}$, in Figures 5a, 5b and 5c we represent its values for three operating conditions. As could be expected, for both refrigerants it can be observed that $\Delta T_{casc.}$ decreases when the mass flow rate is reduced, that is, when the compressor rotation speed is lower, and when the difference between the heat sink and the cold source increases.

In terms of comparing R134a and R152a, the cascade condenser presents a lower $\Delta T_{casc.}$ value when the plant is working with R134a. But, as the temperature difference between the heat sink and the cold source increases, the $\Delta T_{casc.}$ value of R134a comes closer to that of R152a, although it is still lower than that of R152a for the maximum temperature difference.

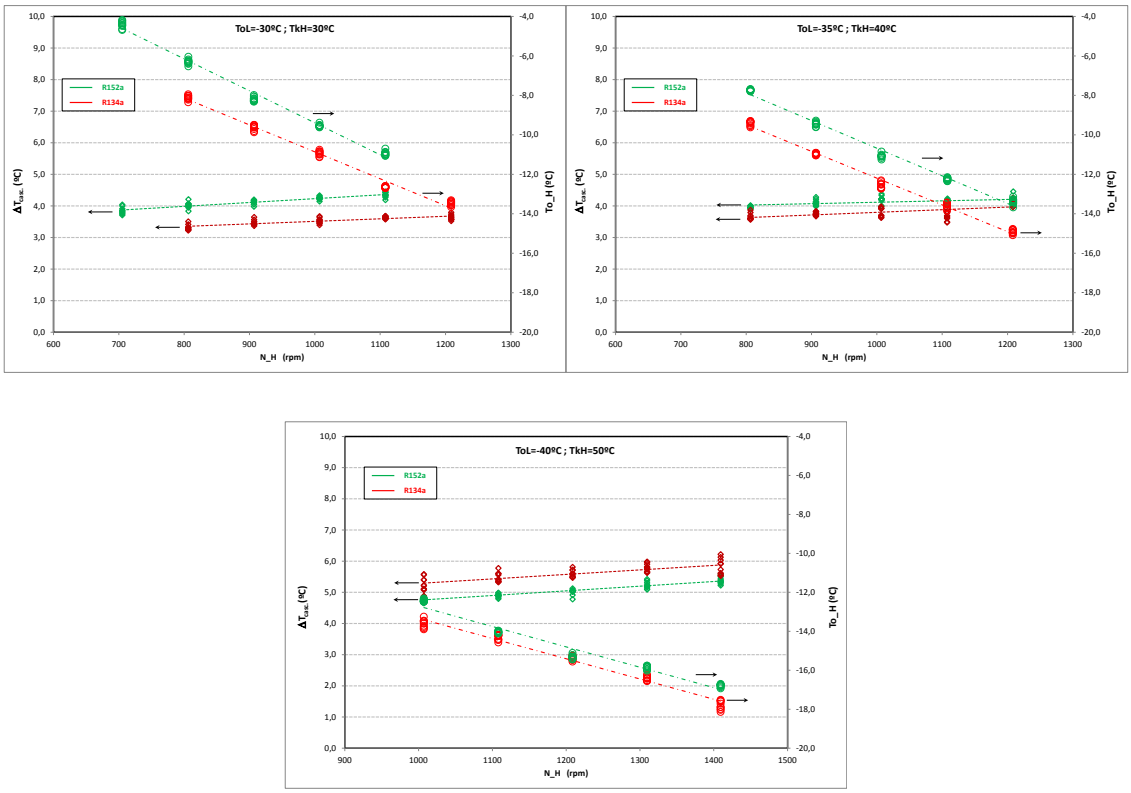

Figures 5a, 5b and 5c. Evolution of $\Delta T_{casc.}$ and T_{oH} with T_{kH}, T_{oL} and N_H evolution for different operating conditions.

The difference in $\Delta T_{casc.}$ when the plant is working with R134a or with R152a, together with the modifications in the compressor speed, are the main variables not considered in the theoretical analysis.

Another parameter represented in Figures 5a, 5b and 5c is the HT evaporating temperature ($T_{o,H}$). For the whole range of $T_{k,H}$ and $T_{o,L}$ tested, the R152a evaporating temperature is between 1 ºC and 2 ºC higher with respect to that of R134a. This fact means that, as the saturation pressures are equal for both refrigerants in the range of evaporating temperatures tested, the HT compressor works with a lower pressure ratio if the facility is charged with R152a than if it is charged with R134a. The variation in HT pressure ratio does not affect that of LT, because the higher $T_{o,H}$ value with R152a is offset by the higher $\Delta T_{casc.}$, resulting in a very similar LT pressure ratio (see Figures 6a and 6b).

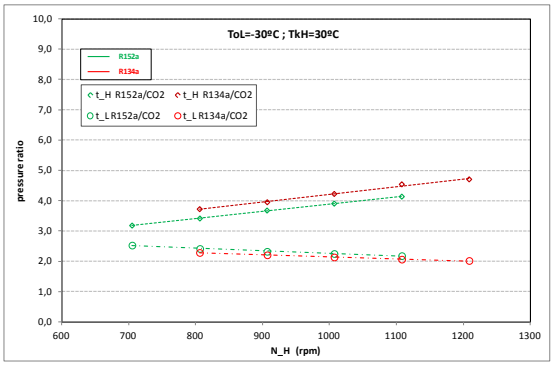

Figure 6a. Pressure ratio in High and Low temperature cycles, working at T_{oL}=-30 ºC and T_{kH}=30 ºC.

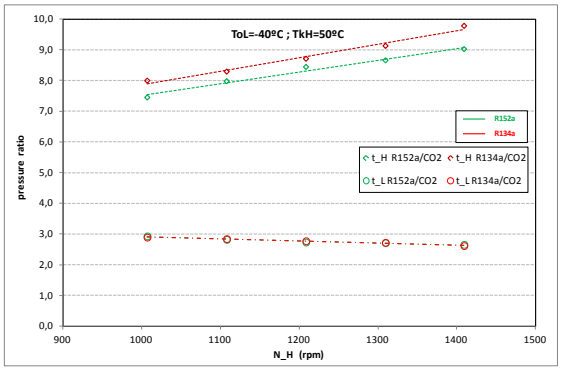

Figure 6b. Pressure ratio in High and Low temperature cycles, working at T_{oL}=-40 ºC and T_{kH}=50 ºC.

In Figures 7a and 7b, the main heat transfer rates obtained at the LT evaporator $(\acute{Q}_{o,L})$, HT condenser $(\acute{Q}_{k,H})$, and Cascade condenser $(\acute{Q}_{k,L})$ are depicted for the two extreme operating conditions tested.

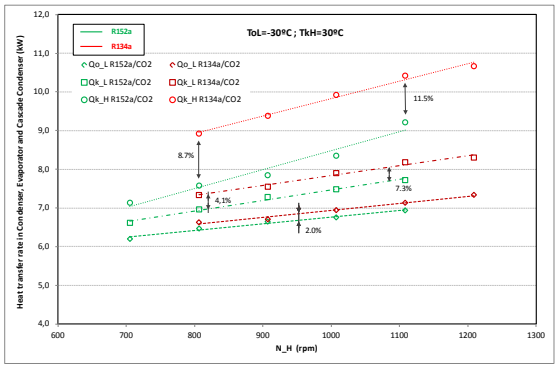

Figure 7a. Main Heat transfer rates in the cascade refrigeration facility at ToL=-30 ºC and TkH=30 ºC.

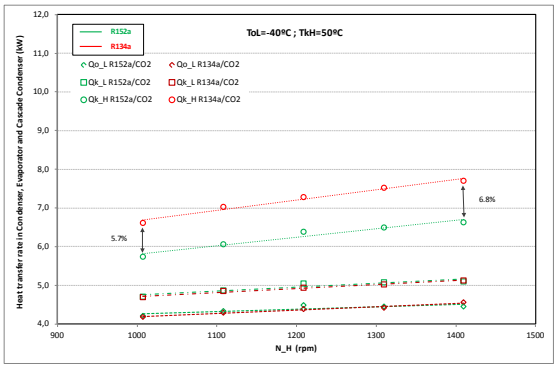

Figure 7b. Main Heat transfer rates in the cascade refrigeration facility at ToL=-40 ºC and TkH=50 ºC.

From the depicted data we can conclude that the utilization of R152a as the working fluid instead of R134a results in lower heat transfer rates. The cooling capacity at the LT evaporator presents the lowest difference, being below 2% over the whole range of operating conditions tested. In contrast, the heat rejected at the HT condenser presents the greatest differences between refrigerants, owing to the cumulative effect of the power consumption differences at the compressors and the heat absorbed at the evaporator and the cascade condenser.

Taking into account the differences in refrigerant mass flow rates in the HT cycle and those in the heat transfer rates, the greater latent heat of evaporation and condensation of R152a with respect to that of R134a plays an important role in equalizing the energy behavior of the cascade plant when R134a is replaced with R152a.

The gas-cooler placed following the compressor discharge in the LT cycle (see Figure 3) rejects a considerable amount of heat to the environment (around 1kW, depending on the environmental temperature). This is why the difference between heat transfer rates at evaporation and condensation levels in the LT cycle is much lower than in the HT cycle, for both refrigerants R134a and R152a.

The power consumption of the two compressors and their corresponding global efficiency, calculated according to Equation 19, are shown in Figures 8a and 8b for the minimum and maximum temperature difference of the heat sink and the cold source.

$$\eta_G = \frac{\acute{m}_{ref.} \cdot w_{cs}}{P_c} \qquad \text{eq. (19)}$$

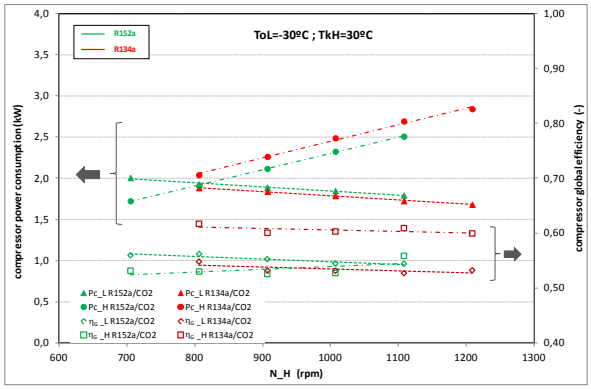

Figure 8a. Power consumption and global efficiency of compressors at ToL=-30 ºC and TkH=30 ºC.

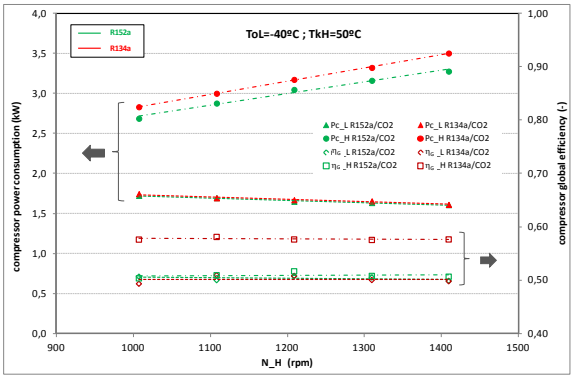

Figure 8b. Power consumption and global efficiency of compressors at ToL=-40 ºC and TkH=50 ºC.

The power consumption measured in the CO2 compressor is practically the same regardless of whether R134a or R152a is used in the HT cycle, while the HT cycle compressor consumes less power when the refrigeration plant uses R152a as the working fluid than if it uses R134a.

Notwithstanding, a poorer global efficiency (between 5% and 8%) is revealed when the compressor mounted in the HT cycle works with R152a in comparison to that obtained when it works with R134a. Regarding Equation 19, this reduction in efficiency occurs despite the reduction in compressor power consumption and the increase in the isentropic specific compression work. Therefore, we can conclude that the refrigerant mass flow rate is the leading factor that determines the global efficiency.

All the issues commented in this section are summarized in Figure 9, where a Sankey diagram is presented for the cascade refrigeration plant working under fixed conditions. This figure shows the

reduction in heat transfer rates and in compressor power consumption when R152a is the working fluid used in the HT cycle, instead of R134a. Nevertheless the differences are not significant.

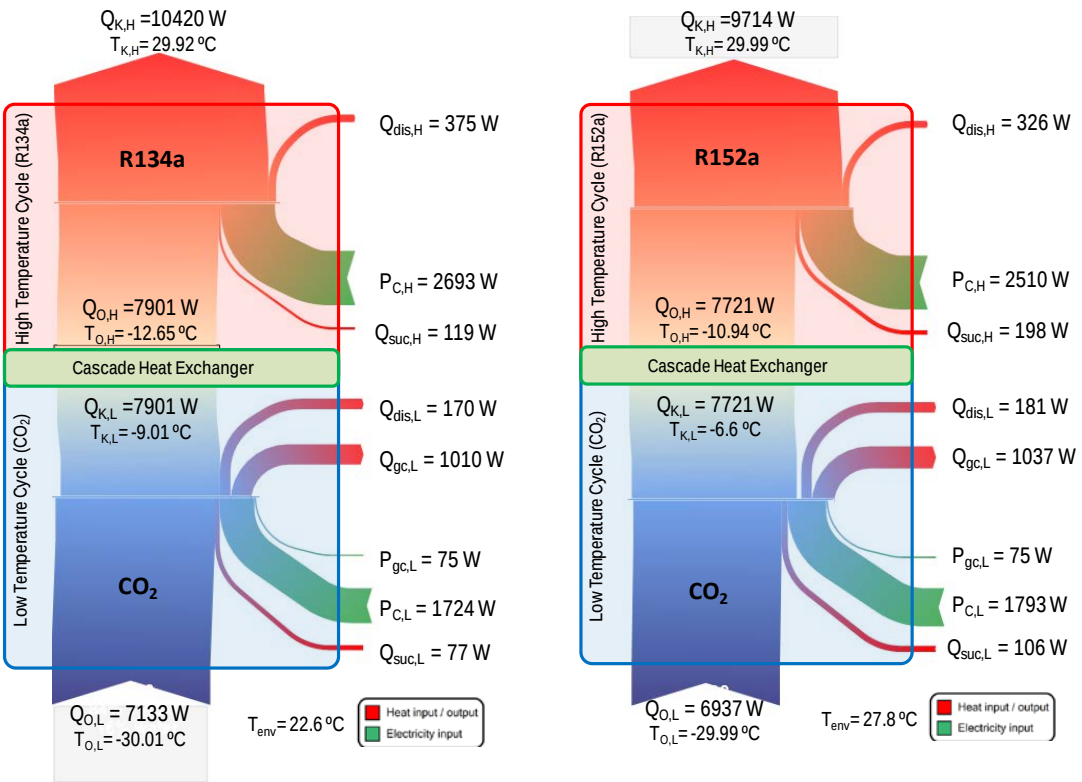

Figure 9. Energy flow through the cascade plant at $T_{o,L}$ = -30.0 ºC, $T_{k,H}$ = 30.0 ºC, N_L = 1450 rpm, N_H =1108 rpm.

The COP of the high and low temperature cycles, COP_{LT} and COP_{HT} respectively, together with the COP of the whole cascade refrigeration facility (COP_T) have been calculated using Equations 20, 21 and 22 respectively, for the minimum and maximum difference in hot and cold temperature sources, in the same way as was already carried out with the other parameters discussed above.

$$COP_L = \frac{\acute{Q}_{0L}}{P_{cL} + P_{gc}} \qquad \text{eq. (20)}$$

$$COP_H = \frac{\acute{Q}_{0H}}{P_{cH}} \qquad \text{eq. (21)}$$

$$COP_T = \frac{\acute{Q}_{0L}}{P_{cL} + P_{gc} + P_{cH}} \qquad \text{eq. (22)}$$

The results obtained are depicted in Figures 10a and 10b. In these figures we can observe that there is no substantial difference between the energy efficiency of the refrigeration facility (COP_T) when working with either of the two refrigerants in the high temperature cycle (R134a or R152a).

Another issue that is observed in Figures 10a and 10b is the independence of COP_T with the compressor speed under both operating conditions and with both refrigerants. This means that regulation using an inverter does not affect the energy performance of the cascade refrigeration plant.

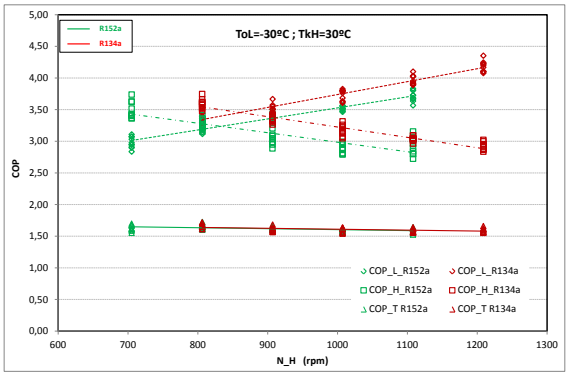

Figure 10a. Energy Efficiency of the HT and LT cycles calculated separately (COP_L and COP_H) and connected in cascade (COP_T) at T_{oL}=-30 ºC and T_{kH}=30 ºC.

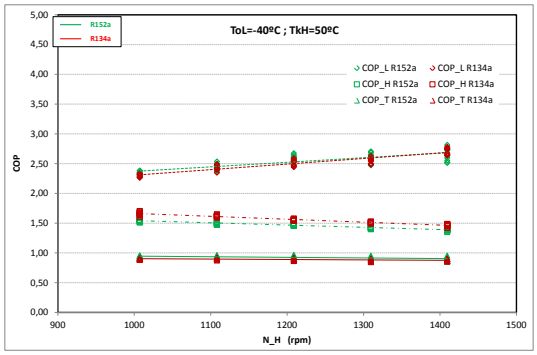

Figure 10b. Energy Efficiency of the HT and LT cycles calculated separately (COP_L and COP_H) and connected in cascade (COP_T) T_{oL}=-40 ºC and T_{kH}=50 ºC.

In general, these results obtained for COP_H agree with those published by R. Cabello et al. (2015) for a single stage vapor compression plant. In that publication, R134a shows better energy performance than R152a for high evaporating temperatures, this difference tending to be reduced until it practically disappears as the evaporating temperature is lowered, which means T_o=-10 ºC.

This section finishes with Tables 6a and 6b, which show a summary of the data collected and the main energy parameters when the refrigeration plant is working at compressor speeds of 1108 rpm and 1007 rpm for the HT cycle compressor, and 1450 rpm for the LT cycle compressor.

One of the parameters shown in these tables is the discharge temperature, which has not been considered so far. From the measured data, an increase in this parameter, ranging from 9 ºC to 15 ºC , can be observed when the HT compressor is working with R152a instead of R134a, this increase. This fact is in agreement with the mass flow rate, because the lower the mass flow rate, the higher the compressor discharge temperature is, as depicted in Figure 11. In the LT cycle there is also an increase in the discharge temperature, due to the lower CO_2 mass flow rate moved by the LT compressor when R152a is working in the HT cycle.

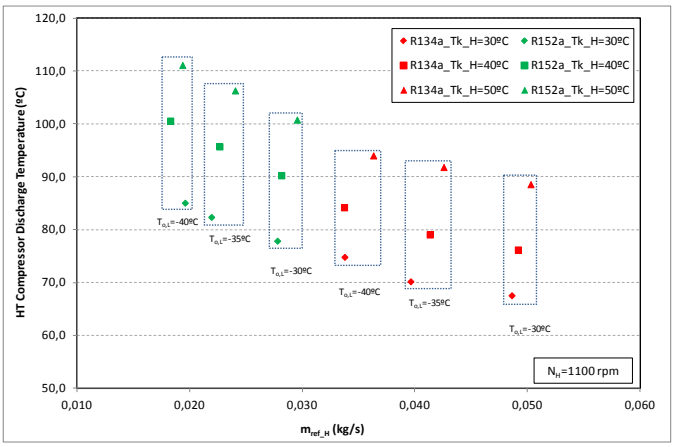

Figure 11. Compressor discharge temperatures versus refrigerant mass flow rate, both in the HT cycle, when the compressor is running at 1100 rpm under different operating conditions.

In general, we can conclude that the results obtained from the experimental data are in accordance with those obtained in the theoretical analysis. The discrepancies lie in the assumptions made in the theoretical study concerning the same ΔT_{casc}, and in considering a different HT compressor displacement for each refrigerant.

7 Conclusions

Using the same cascade refrigeration facility, a full test campaign was carried out covering a wide range of operating conditions: T_{oL} was varied from -30 ºC to -40 ºC, T_{kH} was varied from from 30 ºC to 50 ºC, and the HT cycle compressor speed was varied from 800 rpm to 1400 rpm. These operating conditions were tested using R134a and R152a as the working fluids in the HT cycle, and CO2 as the refrigerant pair for both cases in the LT cycle.

The refrigeration plant is designed for the refrigerant pair R134a/CO2, and a drop-in replacement of R134a with R152a was performed, which involves no changes or substitution of equipment or lubricant, only the adjustment of internal parameters in the electronic expansion valve for a proper regulation.

The refrigeration plant worked correctly for two months using R152a as the refrigerant in the high temperature cycle. This fact confirms the feasibility of using this working fluid in the HT cycle of cascades.

In general, for the same operating conditions, the energy behaviour of the plant does not show great differences when it is working with any of the two refrigerants. It could be highlighted that the results are slightly better for R134a, when the temperature difference between hot and cold source are lower, but as this difference becomes greater, the cascade refrigeration plant, presents better energy results when works with R152a. The discharge temperatures measured at the HT cycle compressor are between 10 ºC

and 15 ºC higher when the working fluid is R152a. This rise supposes that discharge temperature reach in some tests 120ºC, what implies the need of a lubricant of higher quality.

This work presents a comparative analysis from an energy and technical point of view, leaving aside security and cost issues regarding the flammability of R152a, the refrigerant charge needed, and the market price of both refrigerants.

8. Acknowledgments

The authors gratefully acknowledge the financial support for the present work provided by the Spanish Ministry of Economy and Competitiveness (research project ENE2014-53760-R)

9. References

AREA, 2011. Low GWP Refrigerants Guidance on use and basic competence requirements for contractors June 2011
http://www.area-eur.be/_Rainbow/Documents/AREA+-+PP+Low+GWP+refrigerants+(110629).pdf

Arora, S.C. Kaushik Theoretical analysis of a vapour compression refrigeration system with R502, R404A and R507A Int. J. Refrigeration, 31 (2008), pp. 998–1005

ASHRAE Handbook CD, 2001 Edition, American Society of Heating, Refrigerating and Air Conditioning Engineers, Englewood, Colorado (USA), 2001.

ASHRAE, 2013. Designation and Safety Classification of Refrigerants, Standard 34-2013. ISSN:1041-2336. 2013

C. Sanz-Kock, R. Llopis, D. Sánchez, R. Cabello, E. Torrella, 2014. Experimental evaluation of a R134a/CO2 cascade refrigeration plant, Applied Thermal Engineering, Volume 73, Issue 1, 5 December 2014, Pages 41-50, ISSN 1359-4311

Calm J. M., 2012. Refrigerant transitions... again. Moving towards sustainability. In: ASHRAE/NIST Conference, 29 – 30 October, Gaithersburg, MD, USA, (http://nccashrae.org/images/meeting/031214/calm_jm__2012._refrigerant_transitions_..._again._ashrae_nist_refrigerants_conference.pdf)

E. Granryd, I. Ekroth, P. Lundqvist, A. Melinder, B. Palm, P. Rohlin, 2009 Refrigerating Engineering KTH, Department of Energy Technology. ISBN: 978-91-7415-415-3

European Commission, 2005. Council of the European Union. Presidency Conclusions – Brussels, 22/23 March 2005.

European Commission, 2014. Regulation (EU) No 517/2014 of the European Parliament and of the Council of 16 April 2014 on fluorinated greenhouse gases and repealing Regulation (EC) No 842/2006.

IPCC, 2013: Climate Change 2013: The Physical Science Basis. Contribution of Working Group I to the Fifth Assessment Report of the Intergovernmental Panel on Climate Change [Stocker, T.F., D. Qin, G.-K. Plattner, M. Tignor, S.K. Allen, J. Boschung, A. Nauels, Y. Xia, V. Bex and P.M. Midgley (eds.)]. Cambridge University Press, Cambridge, United Kingdom and New York, NY, USA, 1535 pp

IPCC, 2014: Climate Change 2014: Synthesis Report. Contribution of Working Groups I, II and III to the Fifth Assessment Report of the Intergovernmental Panel on Climate Change [Core Writing Team, R.K. Pachauri and L.A. Meyer (eds.)]. IPCC, Geneva,Switzerland, 151 pp.

J.M. Calm, 2008. The next generation of refrigerants – historical review, considerations, and outlook International Journal of Refrigeration, 31 (2008), pp. 1123–1133

Kauffeld, Michael. 2008. “Trends and Perspectives in Supermarket Refrigeration.” International Technical Meeting on HCFC phase-out 05/04/2008. . The Directorate-General for Climate Action. Available online at: http://ec.europa.eu/clima/events/articles/0007_en.htm Accessed October 30, 2015.

Lemmon E. W., Huber M. L., McLinden M. O., 2013. Reference fluid thermodynamic and transport properties (REFPROP), NIST Standard Reference Database 23, v.9.1. National Institute of Standards 2013. Gaithersburg MD, USA.

Law, 2013. Ley 16, 2013, de 29 de octubre, por la que se establecen determinadas medidas en materia de fiscalidad medioambiental y se adoptan otras medidas tributarias y financieras. https://www.boe.es/buscar/act.php?id=BOE-A-2013-11331.

M. Beshr, V. Aute, V. Sharma, O. Abdelaziz, B. Fricke, R. Radermacher, 2015. A comparative study on the environmental impact of supermarket refrigeration systems using low GWP refrigerants. International Journal of Refrigeration, Volume 56, August 2015,Pages 154-164

M. Meinshausen, N. Meinshausen, W. Hare, S. C. B. Raper, K. Frieler, R. Knutti, D. J. Frame and M. R. Allen, 2009. "Greenhouse-gas emission targets for limiting global warming to 2°C." Nature 458(7242): 1158

M. Mohanraj, S. Jayaraj, C. Muraleedharan, 2009. Environment friendly alternatives to halogenated refrigerants—a review Int. J. Greenh. Gas Control, Volume 3, pp. 108–119

O. Abdelaziz, B. Fricke, E. Vineyard, 2012. Development of low global warming potential refrigerant solutions for commercial refrigeration systems using a life cycle climate performance design tool. In: 14th International Refrigeration and Air Conditioning Conference. Purdue University, West Lafayette, Indiana.

R. Cabello, D. Sánchez, R. Llopis, I. Arauzo, E. Torrella. 2015. Experimental comparison between R152a and R134a working in a refrigeration facility equipped with a hermetic compressor, International Journal of Refrigeration, Volume 60, Pages 92-105

R. Llopis, D. Sánchez, C. Sanz-Kock, R. Cabello, E. Torrella. 2015,a. Energy and environmental comparison of two-stage solutions for commercial refrigeration at low temperature: Fluids and systems, Applied Energy, Volume 138, Pages 133-142

R. Llopis, C. Sanz-Kock, R. Cabello, D. Sánchez, E. Torrella. 2015,b. Experimental evaluation of an internal heat exchanger in a CO2 subcritical refrigeration cycle with gas-cooler, Applied Thermal Engineering, Volume 80, Pages 31-41

R. Llopis, C. Sanz-Kock, R. Cabello, D. Sánchez, L. Nebot-Andrés, J. Catalán-Gil. 2016. Effects caused by the internal heat exchanger at the low temperature cycle in a cascade refrigeration plant, Applied Thermal Engineering, Available online 19 April 2016

RD, 2013. Royal Decree 1042/2013, dated 27 December, which passes the Fluorinated Greenhouse Gases Tax Regulation, and which modifies the Regulation of the Procedure for the exercise of disciplinary power, approved by Royal Decree 1398/1993, dated 4 August, the Corporation Tax Regulation, passed by Royal Decree 1777/2004, dated 30 July, the Income Tax Regulation, approved by Royal Decree 439/2007, dated 30 March, and the Value Added Tax Regulation, approved by Royal Decree 1624/1992, dated 29 December. (Official State Gazette, 30-December-2013

Vishaldeep Sharma, Brian Fricke, Pradeep Bansal, 2014. Comparative analysis of various CO2 configurations in supermarket refrigeration systems, International Journal of Refrigeration, Volume 46, October 2014, Pages 86-99,

W.B. Gosney, 1982. Principle of refrigeration. Cambridge University Press. ISBN: 0521236711

W. Goetzler, T. Sutherland, M. Rassi, J. Burgos, 2014. Research & Development Roadmap for Next-Generation Low Global Warming Potential Refrigerants, November 2014, Prepared by Navigant Consulting, Inc for U.S. Department of Energy Office of Energy Efficiency and Renewable Energy Building Technologies Office http://www.energy.gov/eere/buildings/downloads/research-development-roadmap-next-generation-low-global-warming-potential

Figures

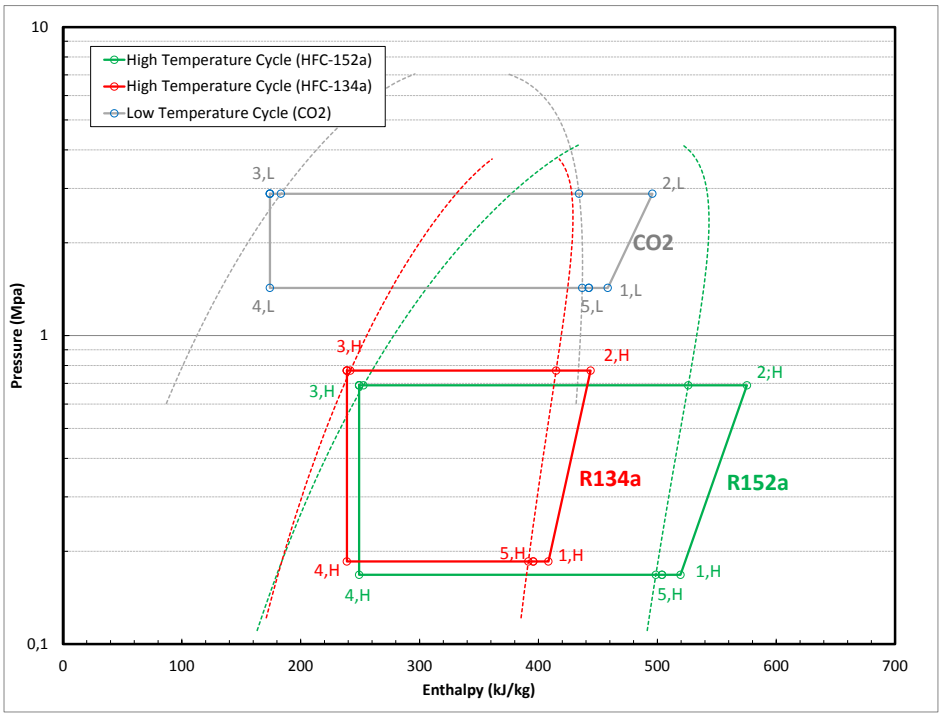

Figure 1. Comparison of the theoretical cascade cycles for R134a/R744 and R152a/R744

Figure 2. View of the cascade refrigeration plant

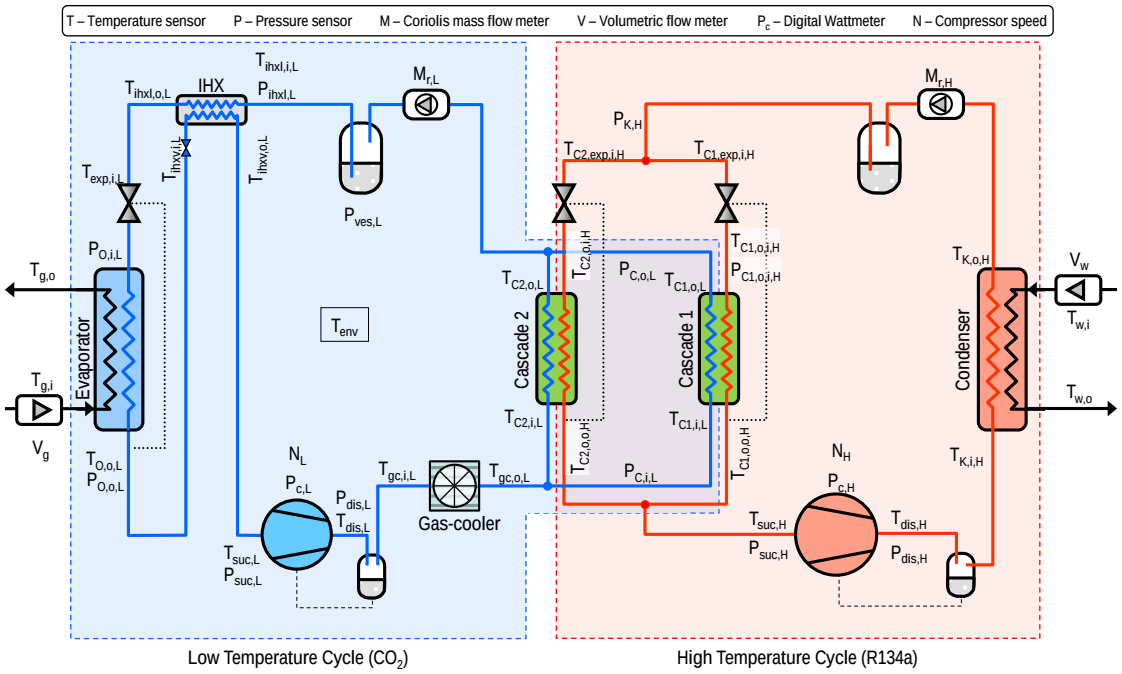

Figure 3. Schematic diagram of the experimental plant

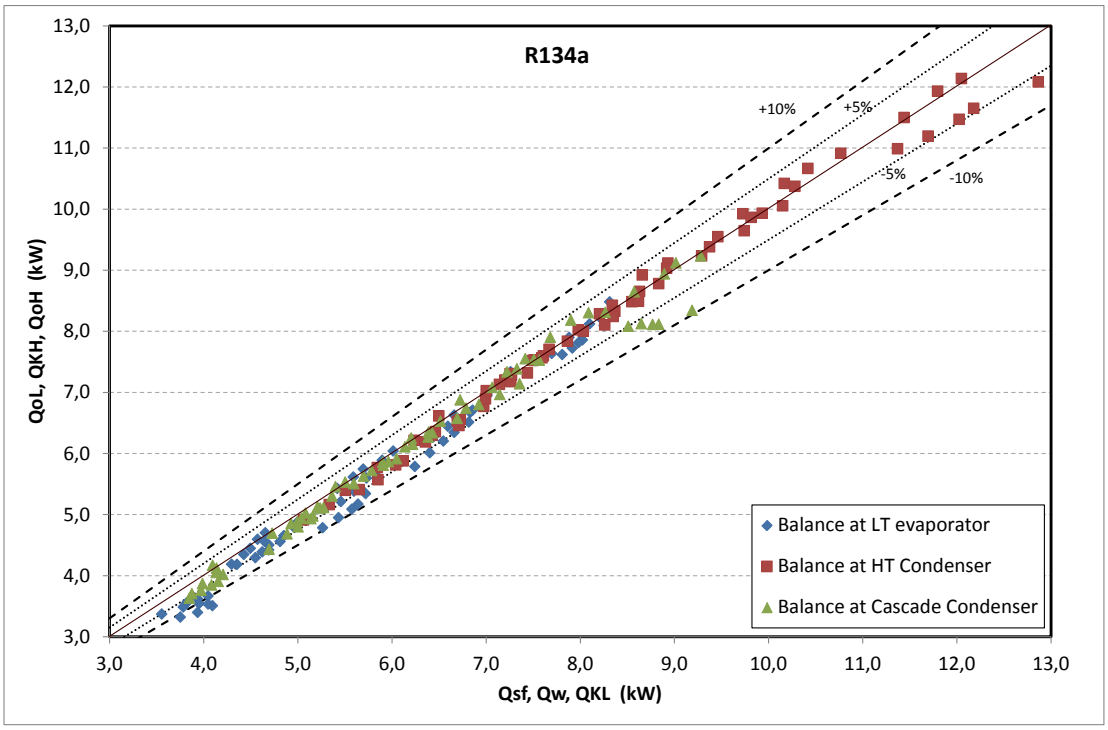

Figure 4a. Validation of heat transfer rates in the cascade plant using R134a/R744

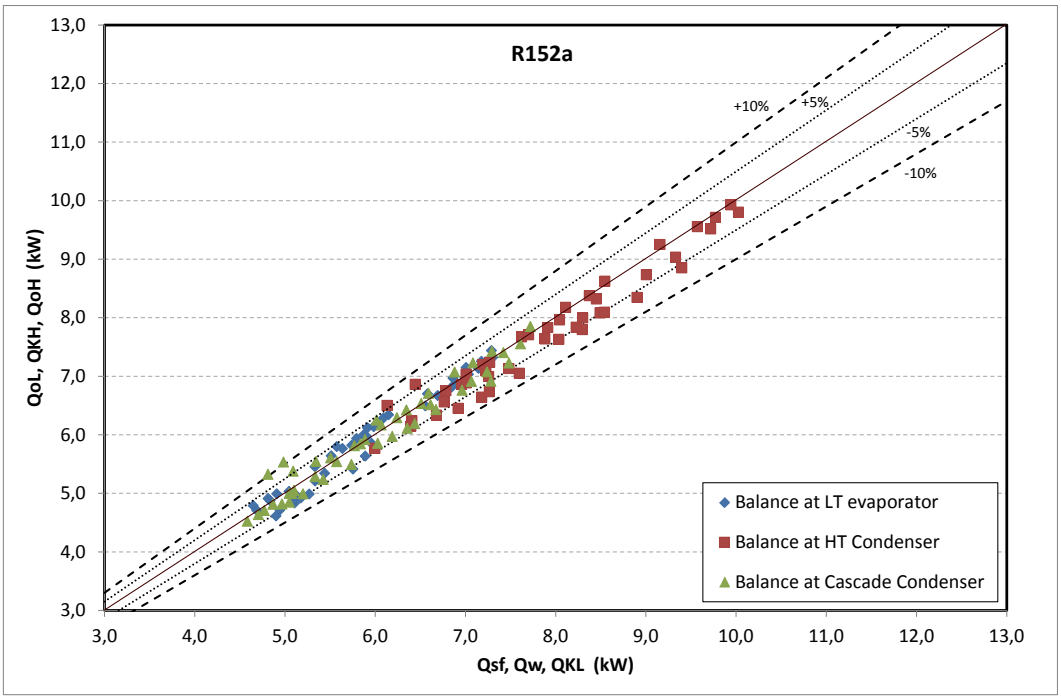

Figure 4b. Validation of heat transfer rates in the cascade plant using R152a/R744

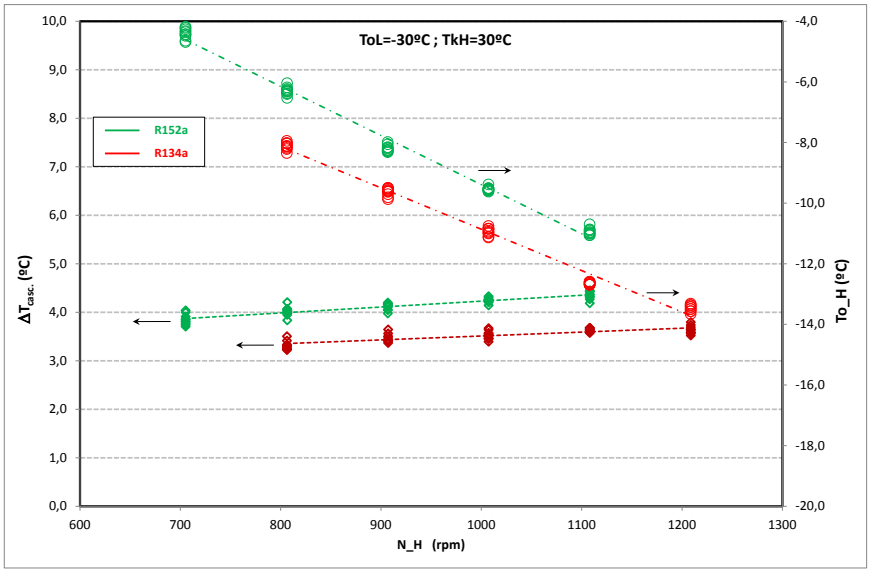

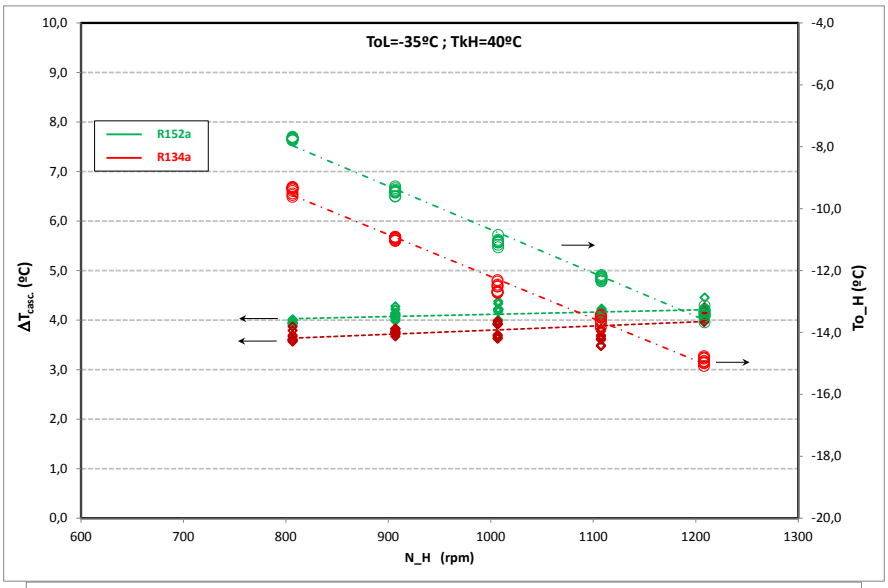

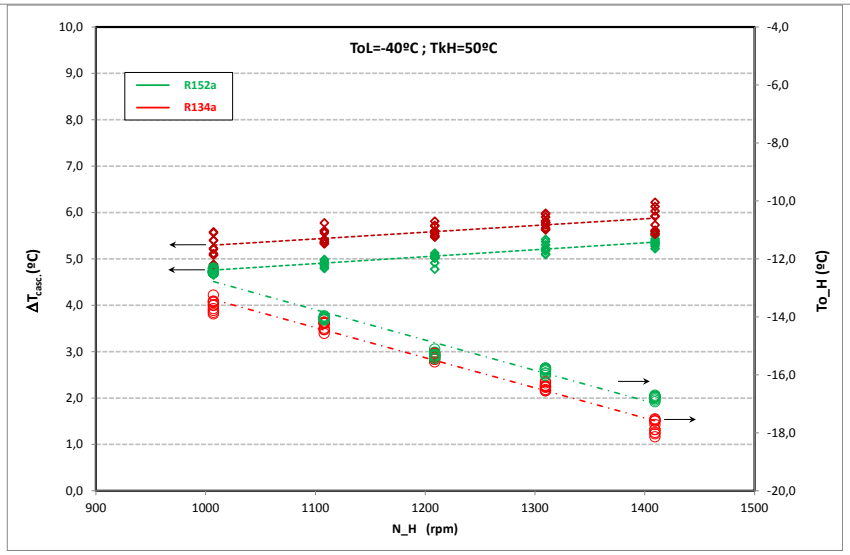

Figures 5a, 5b y 5c. $\Delta T_{casc.}$ y T_{kL} con T_{kH}, T_{oL} y N_H evolution for different operating conditions

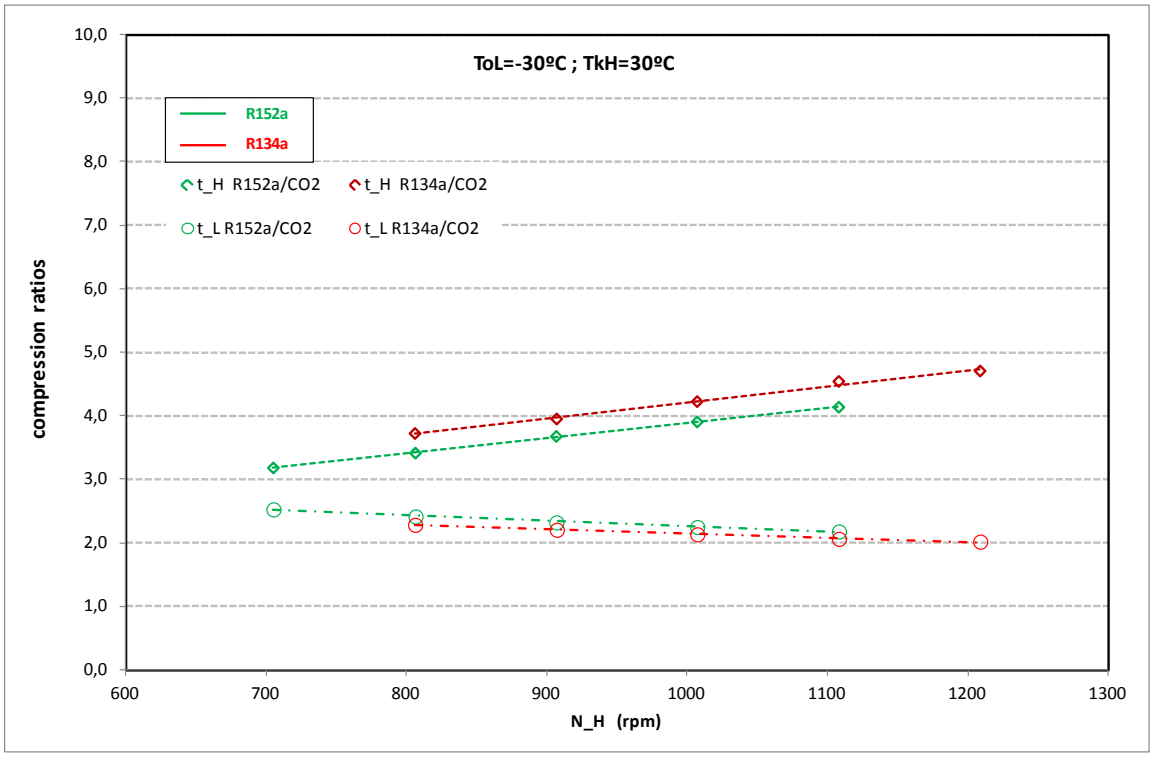

Figure 6a. Pressure Ratio in High and Low temperature cycles, working at ToL=-30ºC and TkH=30ºC

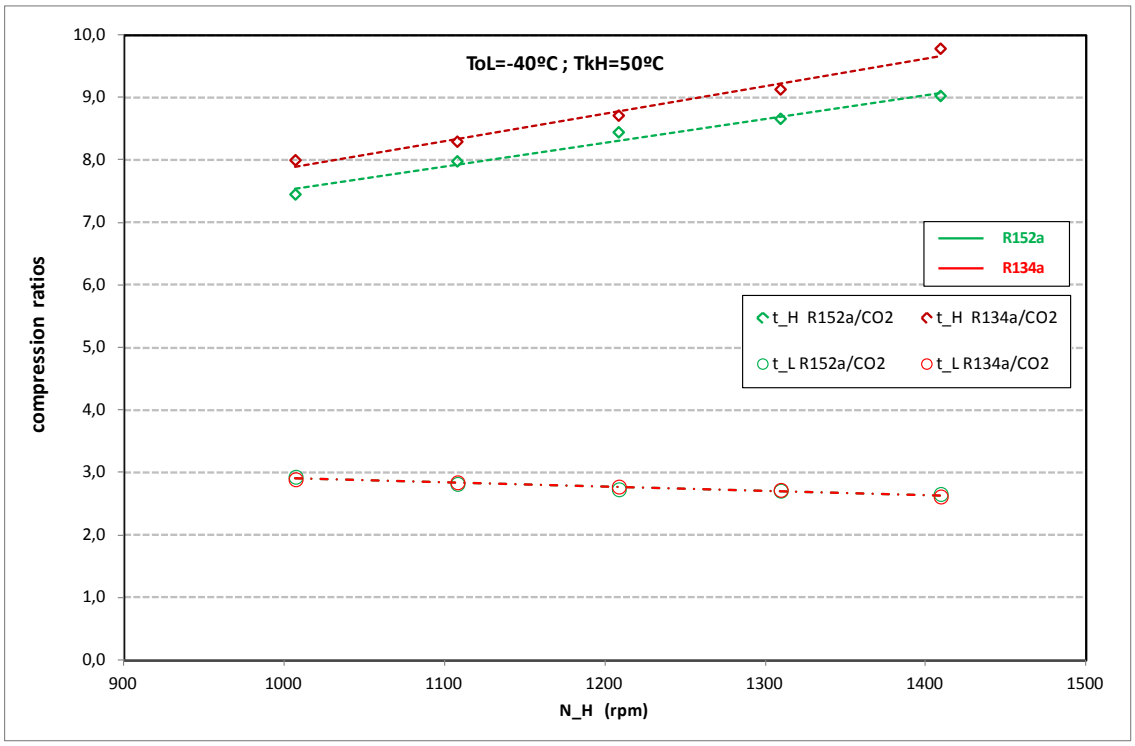

Figure 6b. Pressure ratio in High and Low temperature cycles, working at ToL=-40ºC and TkH=50ºC

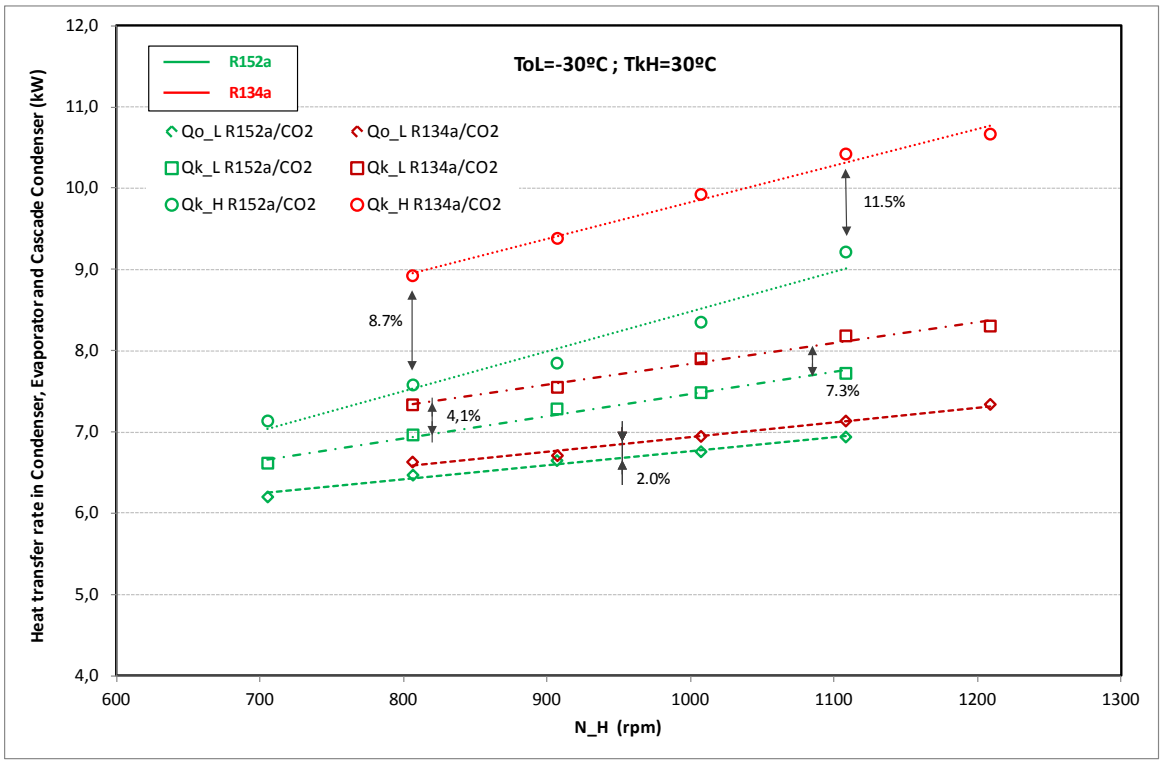

Figure 7a. Main Heat transfer rates in cascade refrigeration facility at ToL=-30ºC and TkH=30ºC

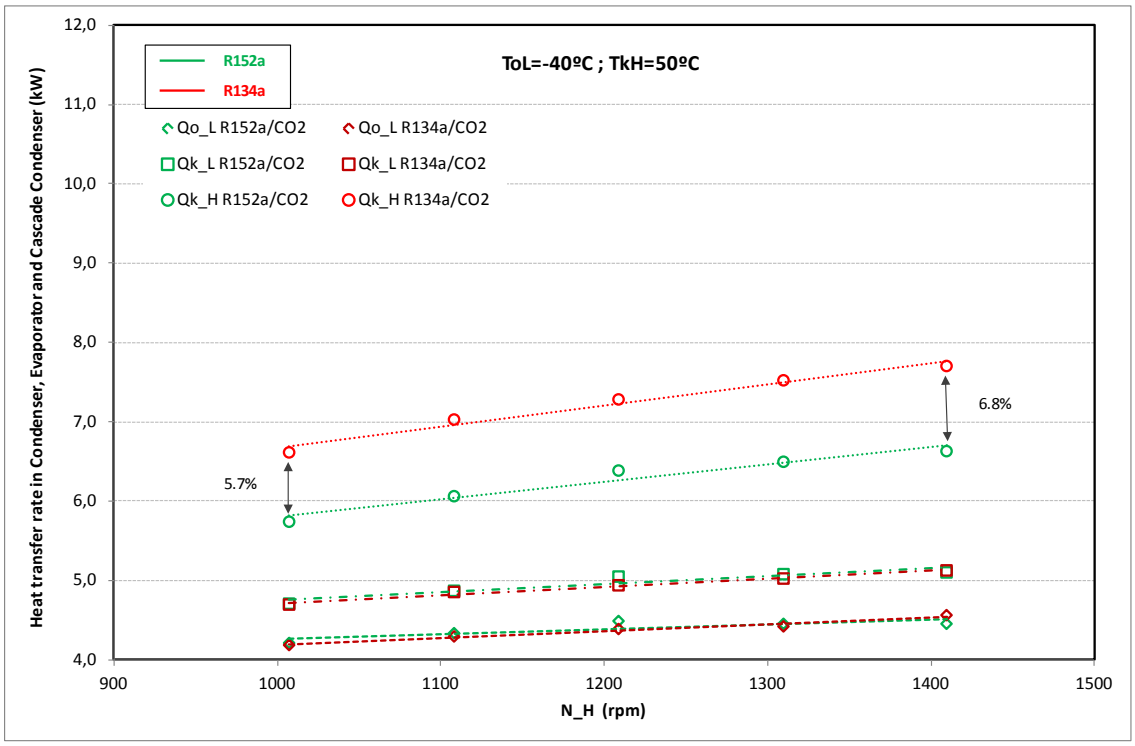

Figure 7b. Main Heat transfer rates in cascade refrigeration facility at ToL=-40ºC and TkH=50ºC

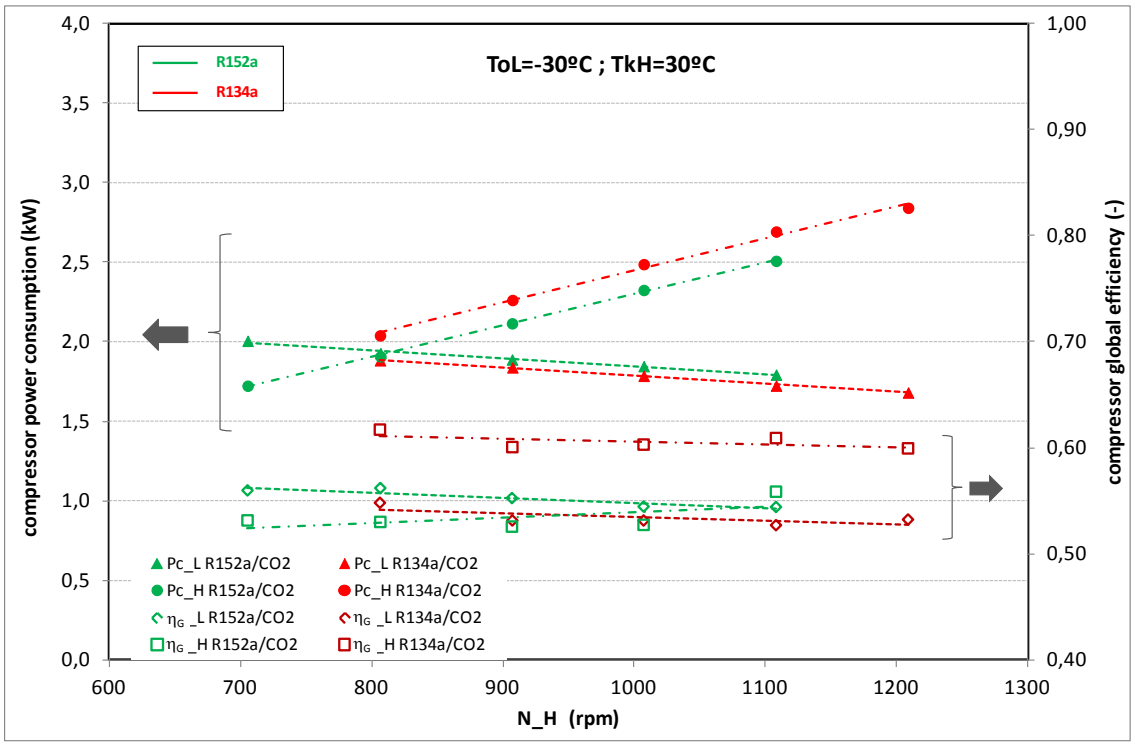

Figure 8a Compressors power consumption and global efficiency at ToL=-30ºC and TkH=30ºC

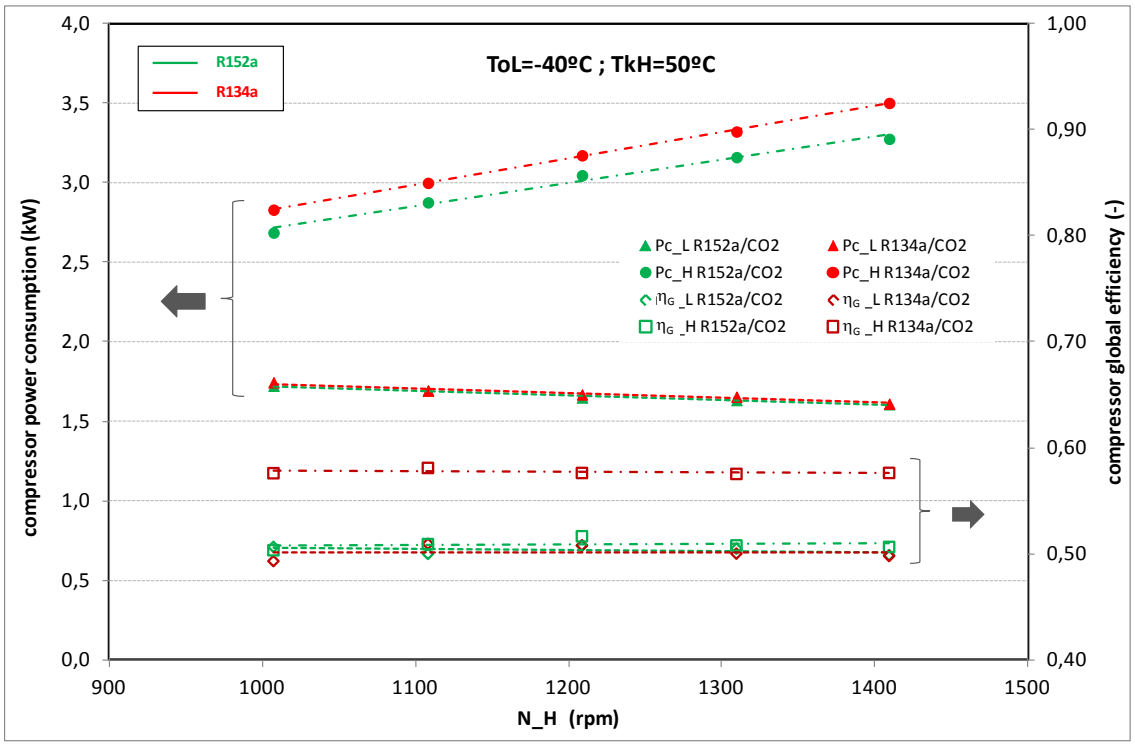

Figure 8b Compressors power consumption and global efficiency at ToL=-40ºC and TkH=50ºC

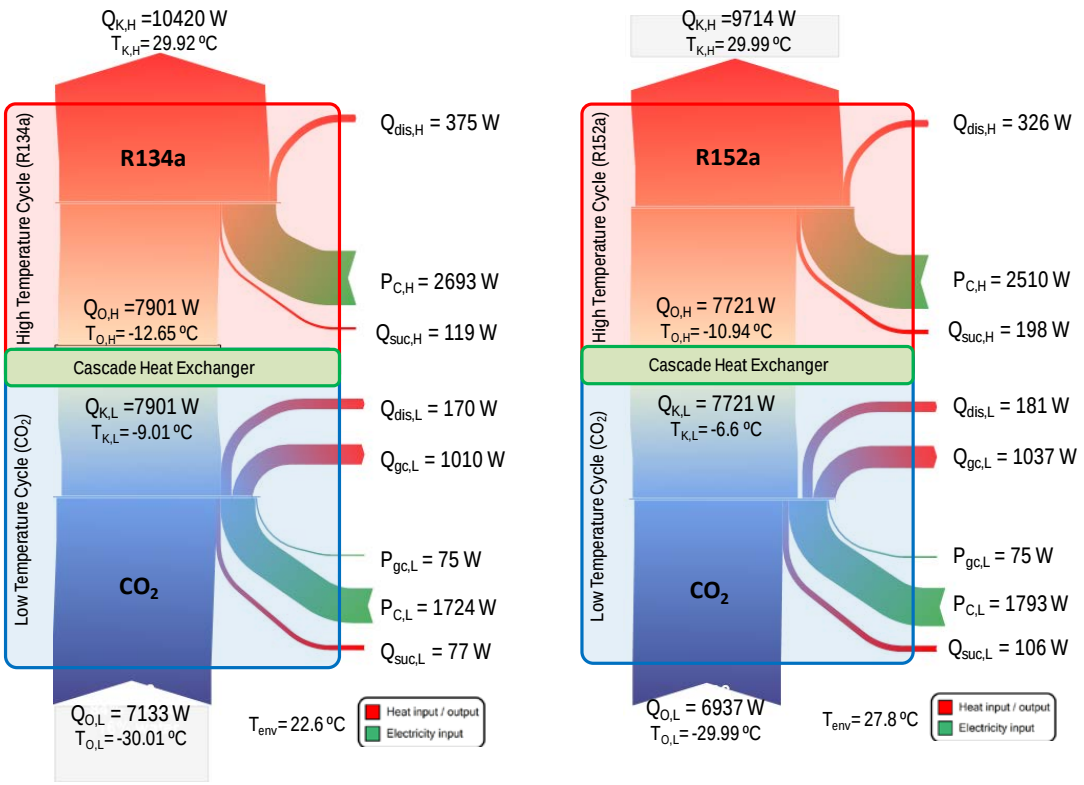

Figure 9. Energy flow through the cascade plant at $T_{O,L}$ = -30.0 ºC, $T_{K,H}$ = 30.0 ºC, N_L = 1450 rpm, N_H =1108 rpm

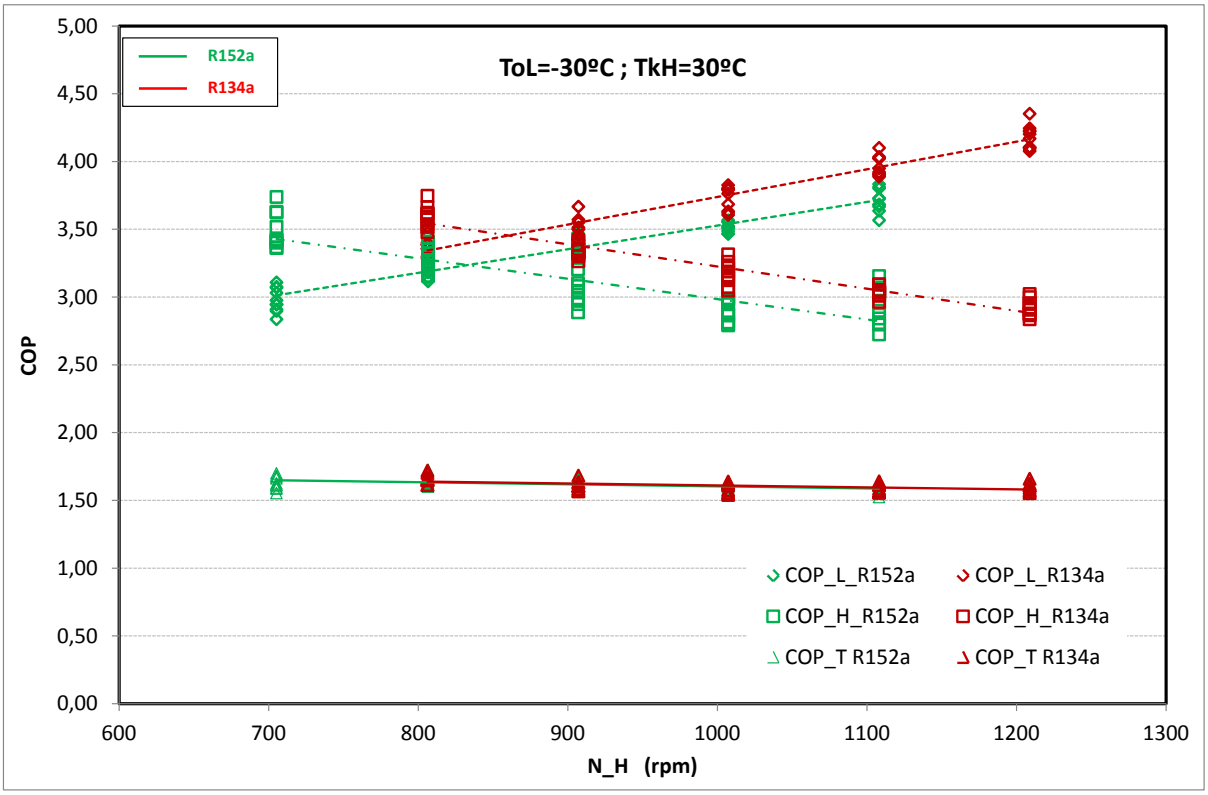

Figure 10a Energy Efficiency of the HT and LT cycles calculated separately (COP_L and COP_H) and connected in cascade (COP_T) at ToL=-30ºC and TkH=30ºC

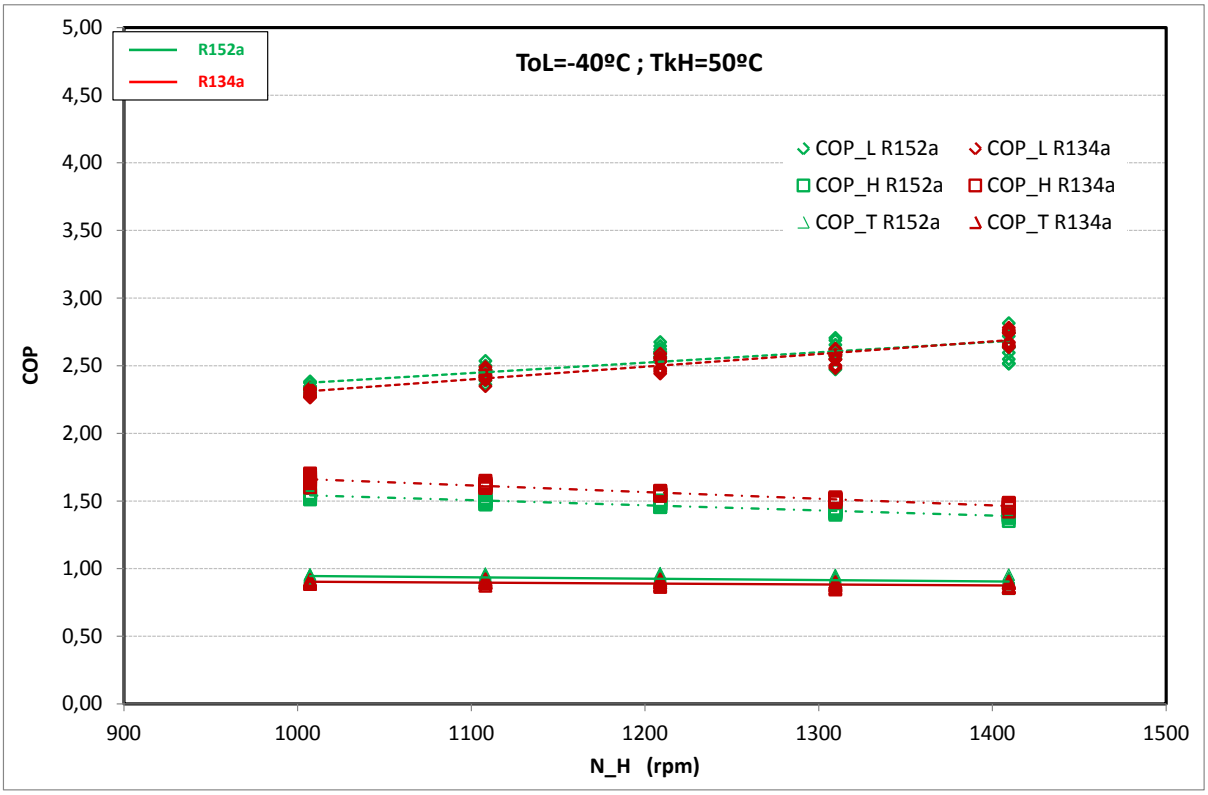

Figure 10b Energy Efficiency of the HT and LT cycles calculated separately (COP_L and COP_H) and connected in cascade (COP_T) ToL=-40ºC and TkH=50ºC

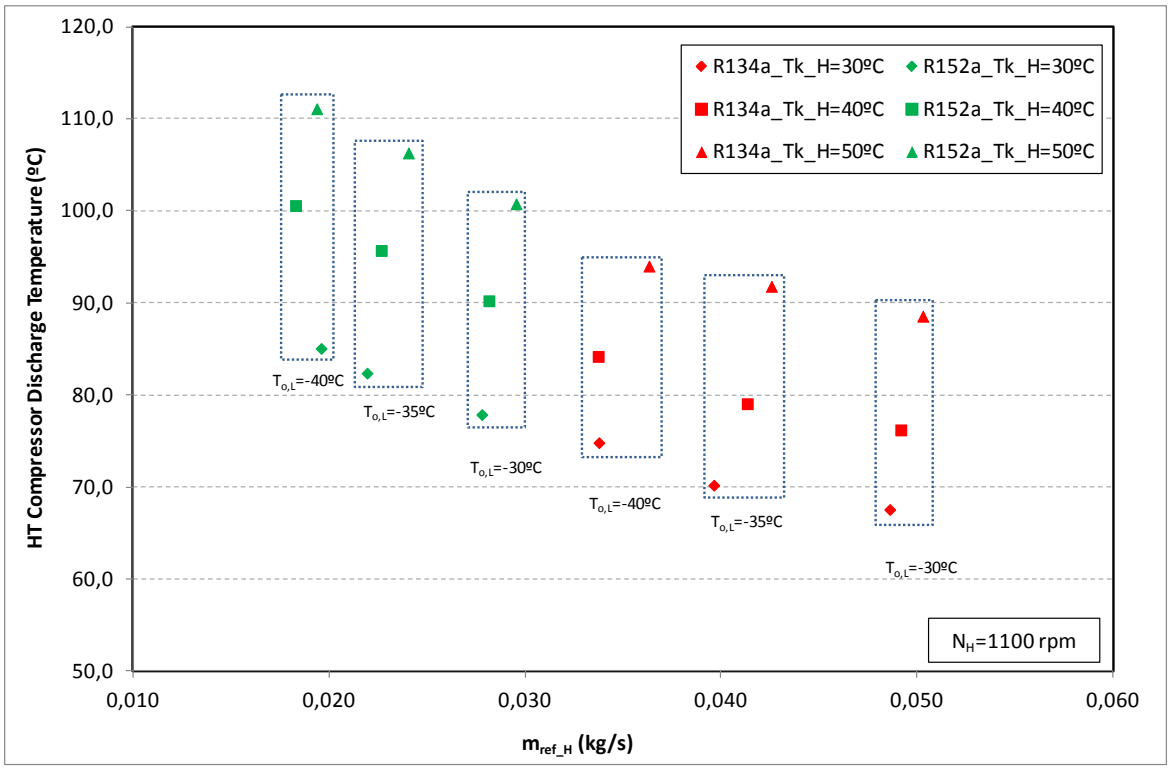

Figure 11. Compressor discharge temperatures versus refrigerant mass flow rate, both in HT cycle, when the compressor is running at 1100 rpm in different operating conditions.

Fluid	Chemical formula	P_{crit} (MPa)	T_{crit} (ºC)	MW ($kg \cdot kmol^{-1}$)	NBP (ºC)	$v_{sat,v}$* ($m^3 \cdot kg^{-1}$)	λ* ($kJ \cdot kg^{-1}$)	qv* ($kJ \cdot m^{-3}$)	Safety Group	RCL ($gr \cdot m^{-3}$)	HOC ($MJ \cdot kg^{-1}$)	GWP[1] WGI-AR5[1]
R152a	CH_3CHF_2	4.52	113.26	66.051	-24.02	0.296	329.91	1113.66	A2	32	17,4	138
R134a	CH_2FCF_3	4.06	101.06	102.032	-26.07	0.190	216.97	1140.81	A1	210	4.2	1300

[1]Working Group I contribution to the IPCC Fifth Assessment Report

*property calculated at NBP

Table 1 – Main thermodynamic, safety and environmental properties of R134a and R152a

High Temperature Cycle (HTC)		Low Temperature Cycle (LTC)	
Working Fluid	HFC134a	Working Fluid	R744 (CO_2)
	HFC152a	Evaporating temperature T_{OL} (ºC)	-30
Condensing temperature T_{KH} (ºC)	30	Condensing temperature T_{KL} (ºC)	-7
Superheat at evaporator outlet (K)	5	Superheat at evaporator outlet (K)	5
Subcooling at expansion valve inlet (K)	2	Subcooling at expansion valve inlet (K)	2
Superheat at compressor suction (K)	15	Superheat at compressor suction (K)	15
Isentropic efficiency $\eta_i = 1 - 0{,}02 \cdot {p_k}/{p_o}$		Isentropic efficiency $\eta_i = 1 - 0{,}04 \cdot {p_k}/{p_o}$	
Volumetric efficiency $\eta_v = 1 - 0{,}02 \cdot {p_k}/{p_o}$		Volumetric efficiency $\eta_v = 1 - 0{,}04 \cdot {p_k}/{p_o}$	
Refrigeration load : $\dot{Q}_{OL} = 1\ kW$			
Temperature difference in cascade condenser ($\Delta T_{casc.}$) : 5 ºC			

Table 2. Input data for theoretical simulation.

$q_o = h_5 - h_4$	Eq (1)	$q_v = \frac{q_o}{v_1}$	Eq (2)
$\dot{m}_{ref,L} = \frac{\dot{Q}_{o,L}}{q_{o,L}}$	Eq (3)	$\dot{m}_{ref,H} = \frac{\dot{m}_{ref,L} \cdot (h_{2L} - h_{3L})}{q_{o,H}}$	Eq (4)
$\dot{V}_G = \frac{\dot{m}_{ref} \cdot v_1}{\eta_v}$	Eq (5)	$w_{c,s} = h_{2s} - h_1$	Eq (6)
$w_c = \frac{h_{2s} - h_1}{\eta_i}$	Eq (7)	$P_c = \dot{m}_{ref} \cdot w_c$	Eq (8)
$t = \frac{p_k}{p_o}$	Eq (9)	$COP_L = \frac{h_{5L} - h_{4L}}{h_{2L} - h_{1L}}$	Eq (10)
$COP_H = \frac{h_{5H} - h_{4H}}{h_{2H} - h_{1H}}$	Eq (11)	$COP_T = \frac{\dot{m}_{ref,L} \cdot (h_{5L} - h_{4L})}{\dot{m}_{ref,L} \cdot (h_{2L} - h_{1L}) + \dot{m}_{ref,H} \cdot (h_{2H} - h_{1H})}$	Eq (12)

Table 3. Equations used in theoretical simulation

Ciclo R152a			Ciclo R134a		
$\dot{m}_{ref,H}$	(kg/s)	0.0047	$\dot{m}_{ref,H}$	(kg/s)	0.0076
$q_{o,H}$	(kJ/kg)	254.7	$q_{o,H}$	(kJ/kg)	156.8
$q_{v,H}$	(kJ/m^3)	1264.4	$q_{v,H}$	(kJ/m^3)	1331.8
$\dot{V}_{G,H}$	(m^3/s)	0.00103	$\dot{V}_{G,H}$	(m^3/s)	0.00098
$w_{c,s,H}$	(kJ/kg)	51.3	$w_{c,s,H}$	(kJ/kg)	32.6
$w_{c,H}$	(kJ/kg)	55.9	$w_{c,H}$	(kJ/kg)	35.5
$Pc,_H$	(W)	263	$Pc,_H$	(W)	271
$T_{dis,H}$	(K/ºC)	342.3 / 69.2	$T_{dis,H}$	(K/ºC)	316.0 / 42.9
t_H	-	4.11	t_H	-	4.15
COP_H	-	3.6	COP_H	-	3.3
Ciclo R744					
$\dot{m}_{ref,L}$	(kg/s)	0.0037			
$q_{o,L}$	(kJ/kg)	268.3			
$q_{v,L}$	(kJ/m^3)	8738.9			
$\dot{V}_{G,L}$	(m^3/s)	0.00012			
$w_{c,s,L}$	(kJ/kg)	33.3			
$w_{c,L}$	(kJ/kg)	37.6			
$Pc,_L$	(W)	140			
$T_{dis,L}$	(K/ºC)	316.6 / 42.9			
t_L	-	2.40			
COP_L	-	5.0			
COP_T	(R152a/CO_2)	2.480	COP_T	(R134a/CO_2)	2.430

Table 4. Energy parameters calculated

$T_{O,L}$ (ºC)	$T_{K,L}$ (ºC)	$\Delta T_{SH,L}$ (ºC)	N_L (rpm)	$T_{O,H}$ (ºC)	$T_{K,H}$ (ºC)	$\Delta T_{SH,H}$ (ºC)	T_{env} (ºC)	N_H (rpm)	Steady-states
-30 ± 0.1	-6.6 to -0.6	9.3 ± 0.2	1450	-10.9 to -4.4	30 ± 0.1	7.4 ± 0.2	27.5 ± 1	705 to 1108	5
-35 ± 0.1	-10.7 to -5.3	9.3 ± 0.1	1450	-15.7 to -9.9	30 ± 0.1	7.7 ± 0.3	26.2 ± 1.8	806 to 1209	5
-40 ± 0.1	-13.2 to -7.9	9.3 ± 0.1	1450	-19.3 to -13.6	30 ± 0.1	8.4 ± 0.3	27.1 ± 1.5	806 to 1209	5
-30 ± 0.1	-6.1 to -1.6	9.2 ± 0.2	1450	-9.6 to -4.2	40 ± 0.1	7.4 ± 0.5	29.9 ± 2	806 to 1209	5
-35 ± 0.1	-9.2 to -3.8	9.2 ± 0.1	1450	-13.4 to -7.7	40 ± 0.1	7.6 ± 0.3	30.0 ± 1.3	806 to 1209	5
-40 ± 0.1	-12.1 to -7.0	9.2 ± 0.1	1450	-17.6 to -11.7	40 ± 0.1	7.8 ± 0.3	29.1 ± 1.6	806 to 1209	5
-30 ± 0.1	-4.6 to 0.9	9.1 ± 0.1	1450	-7.8 to -2.0	50 ± 0.1	7.4 ± 0.2	28.0 ± 1.2	806 to 1209	5
-35 ± 0.1	-7.6 to -2.2	9.1 ± 0.1	1450	-11.6 to -5.7	50 ± 0.1	7.6 ± 0.2	26.7 ± 1.0	806 to 1209	5
-40 ± 0.1	-11.4 to -7.6	9.1 ± 0.1	1450	16.8 to -12.4	50 ± 0.1	7.9 ± 0.2	27.9 ± 1.2	1007 to 1409	5

Table 5a. Summary of the operating conditions kept during tests done with cascade refrigeration plant using R152a

$T_{O,L}$ (ºC)	$T_{K,L}$ (ºC)	$\Delta T_{SH,L}$ (ºC)	N_L (rpm)	$T_{O,H}$ (ºC)	$T_{K,H}$ (ºC)	$\Delta T_{SH,H}$ (ºC)	T_{env} (ºC)	N_H (rpm)	Steady-states
-30 ± 0.1	--4.9 to 0.2	9.0 ± 0.2	1450	-9.17 to -3.43	30 ± 0.1	8.7 ± 0.8	27.5 ± 1.6	907 to 1310	5
-35 ± 0.1	-6.7 to -0.3	9.0 ± 0.2	1450	-11.29 to -3.50	30 ± 0.1	10.0 ± 0.5	26.6 ± 0.9	705 to 1209	5
-40 ± 0.1	-11.5 to -4.8	9.0 ± 0.2	1450	-17.10 to -9.52	30 ± 0.1	9.5 ± 1.8	24.3 ± 1.3	806 to 1409	5
-30 ± 0.1	-6.9 to -1.6	9.4 ± 0.4	1450	-10.68 to -5.00	40 ± 0.1	9.5 ± 0.6	21.8 ± 1.3	806 to 1209	5
-35 ± 0.1	-11.0 to -6.3	9.3 ± 0.3	1450	-15.29 to -10.28	40 ± 0.1	9.4 ± 0.5	21.4 ± 1.4	907 to 1310	5
-40 ± 0.1	-12.8 to -8.0	9.3 ± 0.1	1450	-17.96 to -12.49	40 ± 0.1	9.6 ± 0.4	20.7 ± 0.7	806 to 1209	5
-30 ± 0.1	-9.2 to -3.8	9.3 ± 1.1	1450	-12.71 to -7.25	50 ± 0.1	10.5 ± 1.2	22.7 ± 0.7	806 to 1209	5
-35 ± 0.1	-12.2 to -7.2	9.5 ± 0.4	1450	-16.03 to -10.57	50 ± 0.1	9.7 ± 1.1	20.9 ± 1.4	806 to 1209	5
-40 ± 0.1	-15.4 to -10.3	9.4 ± 0.1	1450	-20.15 to -14.43	50 ± 0.1	9.4 ± 0.9	20.0 ± 1.1	806 to 12097	5

Table 5b. Summary of the operating conditions kept during tests done with cascade refrigeration plant using R134a

T_{kH} (ºC)	T_{oL} (ºC)	T_{kL} (ºC)		ΔT_{casc} (ºC)		$\dot{m}_{ref.L}$ (kg/s)		$\dot{m}_{ref.H}$ (kg/s)		$\dot{Q}_{o.L}$ (kW)		P_{cT} (kW)		COP_T (-)		$T_{disc.H}$ (ºC)		$T_{disc.L}$ (ºC)	
		CO2 (R134a)	CO2 (R152a)	R134a	R152a	CO2 (R134a)	CO2 (R152a)	R134a	R152a	CO2 (R134a)	CO2 (R152a)	R134a	R152a	R134a/ CO2	R152a/ CO2	R134a	R152a	CO2 (R134a)	CO2 (R152a)
30.00	-30.00	-9.0	-6.6	3.6	4.3	0.02655	0.0260	0.0486	0.0278	7.134	6.937	4.492	4.38	1.588	1.585	67.6	77.9	65.2	73.8
30.00	-35.00	-11.9	-9.8	3.7	4.9	0.02148	0.0212	0.0396	0.0219	5.889	5.778	4.217	4.15	1.397	1.392	70.2	82.4	73.1	81.2
30.00	-40.00	-14.5	-12.2	4.6	6.0	0.01724	0.0170	0.0338	0.0196	4.802	4.708	3.964	3.93	1.211	1.198x	74.8	85.1	83.2	94.1
40.00	-30.00	-6.7	-5.4	3.6	3.4	0.02597	0.0253	0.0492	0.0282	6.831	6.690	4.914	4.82	1.390	1.388	76.2	90.2	71.7	78.3
40.00	-35.00	-9.9	-8.1	3.7	4.1	0.02112	0.0204	0.0413	0.0227	5.699	5.502	4.624	4.51	1.232	1.219	79.1	95.7	77.8	88.7
40.00	-40.00	-12.4	-10.5	5.0	5.3	0.01677	0.0162	0.0337	0.0183	4.593	4.418	4.328	4.23	1.061	1.044	84.2	100.6	92.0	101.2
50.00	-30.00	-3.3	-3.3	4.1	3.1	0.02486	0.0247	0.0503	0.0295	6.345	6.472	5.472	5.29	1.160	1.223	88.6	100.8	85.7	85.1
50.00	-35.00	-6.1	-6.2	4.8	3.9	0.01986	0.0199	0.0426	0.0240	5.171	5.320	5.138	4.93	1.007	1.080	91.8	106.3	95.7	95.7
50.00	-40.00	-8.8	-9.2	5.5	4.9	0.01616	0.0160	0.0363	0.0194	4.292	4.333	4.766	4.65	0.901	0.933	94.0	111.1	105.3	106.2

Table 6a. Data summary of the tests carried out at the compressors speeds: N_L=1450 rpm and N_H=1108rpm

T_{kH} (ºC)	T_{oL} (ºC)	T_{kL} (ºC)		ΔT_{casc} (ºC)		$\dot{m}_{ref.L}$ (kg/s)		$\dot{m}_{ref.H}$ (kg/s)		$\dot{Q}_{o.L}$ (kW)		P_{cT} (kW)		COP_T (-)		$T_{disc.H}$ (ºC)		$T_{disc.L}$ (ºC)	
		CO2 (R134a)	CO2 (R152a)	R134a	R152a	CO2 (R134a)	CO2 (R152a)	R134a	R152a	CO2 (R134a)	CO2 (R152a)	R134a	R152a	R134a/ CO2	R152a/ CO2	R134a	R152a	CO2 (R134a)	CO2 (R152a)
30.00	-30.00	-7.4	-5.3	3.5	4.2	0.0262	0.0255	0.0468	0.0254	6.9	6.8	4.35	4.25	1.597	1.591	65.7	75.4	70.0	78.9
30.00	-35.00	-10.9	-8.3	3.7	4.9	0.0211	0.0207	0.0380	0.0222	5.7	5.6	4.10	4.02	1.401	1.397	69.2	80.0	77.9	87.1
30.00	-40.00	-13.3	-10.9	4.7	5.9	0.0169	0.0164	0.0316	0.0189	4.6	4.5	3.84	3.82	1.210	1.176	72.9	82.0	88.3	98.7
40.00	-30.00	-5.5	-3.9	3.5	3.3	0.0256	0.0249	0.0479	0.0268	6.7	6.5	4.77	4.66	1.399	1.402	74.8	88.1	75.6	83.7
40.00	-35.00	-8.8	-6.9	3.8	4.2	0.0210	0.0200	0.0403	0.0221	5.6	5.4	4.52	4.41	1.238	1.213	77.2	94.0	82.2	92.9
40.00	-40.00	-11.1	-9.6	5.0	5.2	0.0164	0.0161	0.0323	0.0181	4.4	4.4	4.20	4.13	1.059	1.060	82.1	98.3	97.4	104.7
50.00	-30.00	-2.2	-2.1	3.9	3.1	0.0246	0.0243	0.0487	0.0287	6.2	6.3	5.33	5.09	1.163	1.239	86.6	98.2	88.8	89.6
50.00	-35.00	-5.1	-5.3	4.7	3.7	0.0197	0.0198	0.0416	0.0235	5.1	5.3	5.02	4.80	1.014	1.096	90.2	103.8	99.1	98.3
50.00	-40.00	-8.4	-7.6	5.3	4.8	0.0158	0.0157	0.0347	0.0185	4.2	4.2	4.65	4.48	0.900	0.939	91.9	109.9	109.5	112.6

Table 6b. Data summary of the tests carried out at the compressors speeds: N_L=1450 rpm and N_H=1007rpm